

# Alterations of Oropharyngeal Microbiome Reflected Disease Severity and Long-Term Dysbiosis in Patients With COVID-19

**Yongzhao Zhou**

Sichuan University West China Hospital

**Sifen Lu**

Sichuan University West China Hospital

**Mengjiao Li**

Sichuan University West China Hospital

**Minjin Wang**

Sichuan University West China Hospital

**Jinmin Ma**

BGI-Shenzhen: BGI Group

**Yuanchen Mao**

BGI-Shenzhen: BGI Group

**Zhongyi Zhu**

BGI-Shenzhen: BGI Group

**Jiumeng Min**

BGI-Shenzhen: BGI Group

**Jun Xiao**

Sichuan University West China Hospital

**Rong Qiu**

Suining Central Hospital

**Taibing Deng**

Guang'an People's Hospital

**Li Jiang**

Chuanbei Medical College: North Sichuan Medical University

**Jing Zhu**

Mianyang Central Hospital

**Yilan Zeng**

public health clinical center of Chengdu

**Dan Liu**

Sichuan University West China Hospital

**weimin li** (✉ [weimi003@scu.edu.cn](mailto:weimi003@scu.edu.cn))

Sichuan University West China Hospital <https://orcid.org/0000-0003-0985-0311>

**Binwu Ying**

Sichuan University West China Hospital

---

## Research

**Keywords:** oropharynx, microbiome, metatranscriptomics, COVID-19, dysbiosis

**Posted Date:** May 6th, 2021

**DOI:** <https://doi.org/10.21203/rs.3.rs-490714/v1>

**License:**  This work is licensed under a Creative Commons Attribution 4.0 International License.

[Read Full License](#)

---

1 **Alterations of oropharyngeal microbiome reflected disease severity and**  
2 **long-term dysbiosis in patients with COVID-19**

3 Yongzhao Zhou<sup>1#</sup> Sifen Lu<sup>2#</sup> Mengjiao Li<sup>3#</sup> Minjin Wang<sup>3#</sup> Jinmin Ma<sup>4</sup> Yuanchen Mao<sup>5</sup> Zhongyi Zhu<sup>5,12</sup>

4 Jiumeng Min<sup>5</sup> Jun Xiao<sup>1,6</sup> Rong Qiu<sup>7</sup> Taibing Deng<sup>8</sup> Li Jiang<sup>9</sup> Jing Zhu<sup>10</sup> Yilan Zeng<sup>11</sup> Dan Liu<sup>1\*</sup>

5 Binwu Ying<sup>3\*</sup> Weimin Li<sup>1,13\*</sup>

6 \*Correspondence: Dan Liu, Binwu Ying, Weimin Li.

7 #Yongzhao Zhou, Sifen Lu, Mengjiao Li, Minjin Wang contributed equally to this work.

8 Email addresses for the authors: Yongzhao Zhou: [yongzhaozhou@scu.edu.cn](mailto:yongzhaozhou@scu.edu.cn);

9 Sifen Lu: [lusifen@wchscu.cn](mailto:lusifen@wchscu.cn); Mengjiao Li: [limengjiao189@163.com](mailto:limengjiao189@163.com);

10 Minjin Wang: [wang.minjin@look.com](mailto:wang.minjin@look.com); Jinmin Ma: [majinmin@genomics.cn](mailto:majinmin@genomics.cn);

11 Yuanchen Mao: [maoyuanchen@bgi.com](mailto:maoyuanchen@bgi.com); Zhongyi Zhu: [zhuzhongyi@bgi.com](mailto:zhuzhongyi@bgi.com);

12 Jiumeng Min: [minjm@bgi.com](mailto:minjm@bgi.com); Jun Xiao: [xiaojun5244@163.com](mailto:xiaojun5244@163.com);

13 Rong Qiu: [443182163@qq.com](mailto:443182163@qq.com); Taibing Deng: [27180619@qq.com](mailto:27180619@qq.com);

14 Li Jiang: [78389789@qq.com](mailto:78389789@qq.com); Jing Zhu: [zhujing\\_1126@126.com](mailto:zhujing_1126@126.com);

15 Yilan Zeng: [zhyilan991827@163.com](mailto:zhyilan991827@163.com); Dan Liu: [liudan10965@wchscu.cn](mailto:liudan10965@wchscu.cn);

16 Binwu Ying: [yngbinwu@scu.edu.cn](mailto:yngbinwu@scu.edu.cn); Weimin Li: [weimi003@scu.edu.cn](mailto:weimi003@scu.edu.cn).

17 1Department of Respiratory and Critical Care Medicine, Frontier Science Center of Disease

18 Molecular Network, West China Hospital, Sichuan University, Chengdu 610041, China

19 2 Precision Medicine Key Laboratory of Sichuan Province and Precision Medicine Center, West

20 China Hospital, Sichuan University, Chengdu, Sichuan 610041, China

21 3Department of Laboratory Medicine, West China Hospital, Sichuan University, Chengdu, Sichuan

22 610041, China

- 23 4BGI-Shenzhen, Shenzhen, 518083, China
- 24 5BGI PathoGenesis Pharmaceutical Technology, BGI-Shenzhen, Shenzhen 518083, China
- 25 6Department of Respiratory and Critical Care Medicine, People's Hospital of Ganzi Tibetan  
26 Autonomous Prefecture, Ganzi Tibetan Autonomous Prefecture 626000, China
- 27 7Department of Respiratory and Critical Care Medicine, Suining Central Hospital, Suining 629000,  
28 China
- 29 8Department of Respiratory and Critical Care Medicine, Guang'an people's Hospital, Guang'an  
30 638000, China
- 31 9Department of Respiratory and Critical Care Medicine, Affiliated Hospital of North Sichuan  
32 Medical College, Nanchong 637000, China
- 33 10Department of Respiratory and Critical Care Medicine, Mianyang Central Hospital, Mianyang  
34 621000, China
- 35 11Department of general medicine, Public Health Clinical Center of Chengdu, Chengdu 610041,  
36 China
- 37 12 College of Life Sciences, University of Chinese Academy of Sciences, Beijing 100049, China
- 38 13 Lead contact

## 39 **Abstract**

40 **Background:** Recent evidences have shown that gut microbiome of patients  
41 with COVID-19 significantly changes and can reflect the severity of the disease.  
42 And gut microbiota richness was not restored to normal levels after 6-month  
43 recovery. However, *SARS-CoV-2* primarily infects the respiratory tract, few  
44 studies investigate whether the alterations of oropharyngeal microbiome is

45 associated with disease severity in patients with COVID-19, and whether  
46 interferences in microbiome composition, if any, eliminate with clearance of the  
47 *SARS-CoV-2* virus. We employed metatranscriptomic sequencing to analyse  
48 oropharyngeal swabs collected within a week of diagnosis COVID-19 (period  
49 of disease group: PDG) and two months after clearance of the *SARS-CoV-2*  
50 virus (convalescent group: CG) from 47 patients with COVID-19. Meanwhile,  
51 oropharyngeal swabs from 40 healthy subjects were analyzed as healthy  
52 control group (HCG).

### 53 **Results:**

54 Oropharyngeal microbial composition was significantly altered in patients with  
55 COVID-19 compared with healthy controls even two months after clearance of  
56 the *SARS-CoV-2* virus. Little changes in  $\alpha$ -diversity among HCG, PDG and CG  
57 ( $P > 0.05$ ), but obviously changes in  $\beta$ -diversity among them. Notably,  
58 *Prevotella* increased significantly in PDG than that in HCG (Wilcoxon rank-sum  
59 test,  $P < 0.001$ ) and increased gradually along with the severity of patients with  
60 COVID-19 aggravated. There was a positive correlation between *Prevotella*  
61 and the elevation of Neutrophil percentage ( $R = 0.301$ ,  $P = 0.040$ ). Similarly,  
62 *SARS-CoV-2* and *Aspergillus* increased remarkably in critical Patients with  
63 COVID-19. There was a negative correlation between *SARS-CoV-2* viral load  
64 and platelet counts ( $R = -0.330$ ,  $P = 0.022$ ).

65 **Conclusions:** The oropharyngeal microbiome in patients with COVID-19  
66 present persistent dysbiosis even two months after clearance of the *SARS-*

67 CoV-2 virus. Furthermore, alterations in oropharyngeal microbial composition  
68 reflected the severity of disease in patients with COVID-19. Our findings  
69 underscore that there is an urgent need to understand the specific roles of  
70 oropharyngeal microorganisms in COVID-19 disease progression and  
71 rehabilitation.

72 **Keywords:** oropharynx, microbiome, metatranscriptomics, COVID-19,  
73 dysbiosis

74

75

76

77

78

79

80

81

82

83

84

85

86

87

88

89 **Background**

90 The COVID-19 pandemic is a once-in-a-century public health emergency, the  
91 causative pathogen was identified as a virus, named severe acute respiratory  
92 syndrome coronavirus 2 (*SARS-CoV-2*)[1]. Although caused only by the *SARS-*  
93 *CoV-2* virus, COVID-19 is likely affected by the rest of the microbiome as  
94 evidenced by viral persistence in the gut, and risk factors associated with gut  
95 microbial (include bacteria and fungi) dysbiosis[2-5]. Indeed, there is a study  
96 suggesting that the disease severity is concordant with composition alteration  
97 of the gut microbiome in patients with COVID-19, and the dysbiotic gut  
98 microbiota composition in patients with COVID-19 persists after clearance of  
99 the virus[6]. Besides, another study found that microbiota richness was not  
100 restored to normal levels after 6-month recovery[7]. Recently, Microbiome  
101 Centers Consortium has called for researchers try to figure out the connections  
102 between the microbiome and COVID-19[2]. *SARS-CoV-2* primarily infects the  
103 respiratory tract. Study has already shown that low respiratory tract microbiota  
104 in *SARS-CoV-2* infected patients were dominated with elevated levels of the  
105 upper respiratory tract (URT) commensal microbiota[8], unlike *influenza* virus[9-  
106 12], few studies have explored the relationship between *SARS-CoV-2* infection  
107 and the oropharyngeal microbiome. Therefore, we investigated whether the  
108 alterations of oropharyngeal microbiome are associated with disease severity  
109 in patients with COVID-19, and whether interferences in microbiome  
110 composition, if any, eliminate with clearance of the *SARS-CoV-2* virus.

## 111 Results

### 112 Study cohort

113 We recruited 47 patients with COVID-19 confirmed by positive *SARS-CoV-2*  
114 quantitative reverse transcription PCR(RT-qPCR) to establish a longitudinal  
115 cohort study. And we collected oropharyngeal swabs at two time points  
116 (Within a week of diagnosis COVID-19 (period of disease group: PDG) and two  
117 months after clearance of the *SARS-CoV-2* virus (convalescent group: CG))  
118 during February and June 2020. The subjects were classified into mild,  
119 moderate, severe, and critical groups based on symptoms as reported  
120 before[13, 14]. As healthy controls group (HCG), we collected oropharyngeal  
121 swabs from 40 healthy human subjects free of any respiratory infections during  
122 the same timeframe. Clinical information and demographic information were  
123 presented in **Table 1**.

124 **Table 1** Clinical characteristics of participants

	COVID-19 patients (period of disease group / convalescent group)*	healthy controls
Number of subjects	47	40
Gender (females, males)	27, 20	20, 20
Age, years (mean±SD)	44.7±15.3 years	45.8±16.4 years
Disease severity category	5 mild, 25 moderate, 10 severe, 7 critical	NA
Symptoms at admission, n (%)		
Fever	29(61.7%)	NA
Cough	29(61.7%)	NA
Sputum	19(40.4%)	NA
Sore throat	7(14.9%)	NA
Shortness of breath	17(36.2%)	NA

Received antibiotics during first week hospitalisation by disease severity, n (%) <sup>1</sup>		NA
Mild disease	1(2.1%)	NA
moderate disease	3(6.4%)	NA
Severe disease	5(10.5%)	NA
critical disease	7(14.8%)	NA
Received antivirals during first week hospitalisation by disease severity, n (%) <sup>2</sup>		
Mild disease	4(8.5%)	NA
moderate disease	24(51.0%)	NA
Severe disease	10(21.3%)	NA
critical disease	7(14.8%)	NA

125 \* The 47 patients with COVID-19 were longitudinal observed in period of disease and two  
 126 months after clearance of the SARS-CoV-2 virus.

127 <sup>1</sup> The antibiotics included quinolones and cephalosporins.

128 <sup>2</sup> The antivirals included Lopinavir/ritonavir, Ribavirin, Oseltamivir and interferon.

129

130 **The persist dysbiosis of oropharyngeal microbiome in patients with**  
 131 **COVID-19 even two months after clearance of the SARS-CoV-2 virus**

132 We employed metatranscriptomic sequencing in all the 134 oropharyngeal  
 133 swabs to obtain unbiased microbial profiles. In order to remove possible  
 134 contamination, blank control samples, including another 6 swabs not sampled  
 135 were tested. These blank control samples were applied to extract microbial  
 136 genomic nucleotide and were tested using the same batch of consumables and  
 137 reagents in the same equipment and laboratory. Then we analyzed the  
 138 unbiased metatranscriptome sequencing data of 140 samples using a  
 139 database[15] (built by updating all the complete genomes from NCBI Refseq  
 140 database in real time) consisting of 4,409 genera (37,933 species) of bacteria,  
 141 fungi, and viruses for taxonomic classification.

142 **The persist oropharyngeal bacterial dysbiosis:** Overall, 534 unique genera  
 143 of bacteria were detected in oropharyngeal swabs from HCG, PDG and CG.

144 There were 73 genera with relative abundance greater than 0.01% in 534  
145 genera. The relative abundances of the most top20 abundant bacterial profiles  
146 in oropharyngeal swabs from HCG, PDG and CG were shown as **Fig.1a, b, c**,  
147 and top20 abundant bacterial profiles of every subjects were shown as  
148 **Suppl.Fig.1a, b, c**. Among the 534 genera, the PDG, CG and HCG groups  
149 shared with 244 genera and had 63, 36 and 61 unique genera, respectively  
150 (**Fig.1e**); Among the 244 shared genera, *Prevotella* were dominant genera of  
151 the PDG and CG (**Fig.1f**). Consistent with previous researches[16, 17], the  
152 major bacterial genera in HCG were *Actinomyces* (12.1%), *Acetobacter*  
153 (10.9%), *Rothia* (10.4%), *Bacteroides* (9.5%), *Prevotella* (8.8%) (**Fig.1a**).  
154 *Actinomyces* and *Rothia* decreased remarkably in group PDG and CG (**Fig.1d**).  
155 *Prevotella* (18.3%), *Neisseria* (11.0%), *Alloprevotella* (5.5%), and  
156 *Fusobacterium* (4.1%) in PDG were significantly higher than that in HCG  
157 (**Fig.1b and Fig.1d**). Two months after SARS-CoV-2 virus has been cleared,  
158 *Prevotella* (19.4%), *Neisseria* (14.2%), *Alloprevotella* (6.9%), and  
159 *Fusobacterium* (5.1%) in CG were even higher than that in HCG or in PDG  
160 (**Fig.1a, b, c and d**). These results indicated that the bacterial microecology of  
161 oropharynx was obviously disturbed by SARS-CoV-2 infection, and it was hard  
162 to get back to normal even two months after the virus has been cleared.

163 **The persist oropharyngeal fungal dysbiosis:** Overall, 103 unique genera of  
164 fungi were detected in oropharyngeal swabs from HCG, PDG and CG. There  
165 were 57 genera with relative abundance greater than 0.01% in 103 genera. The

166 relative abundances of the most top20 abundant fungal profiles in  
167 oropharyngeal swabs from HCG, PDG and CG were shown as **Fig.2a, b, c**.  
168 top20 abundant fungal profiles of every subjects were shown as **Suppl.Fig.2a,**  
169 **b, c**. The PDG, CG and HCG shared with 40 genera and had 12, 11 and 6  
170 unique genera, respectively (**Fig.2e**); Among the 40 shared genera, *Aspergillus*  
171 were dominant genera of the PDG and CG (**Fig.2f**). The major genera in HCG  
172 were *Malassezia* (16.4%), *Aspergillus* (14.8%), *Clavispora* (14.1%), *Daldinia*  
173 (13.6%), *Kwoniella* (7.7%) (**Fig.2a**). Compared with HCG, *Malassezia*,  
174 *Clavispora* and *Pseudogymnoascus* decreased remarkably in PDG and CG  
175 (**Fig.2d**). *Aspergillus* (20.5%) and *Saccharomyces* (15.7%) in PDG were  
176 significantly higher than that in HCG (**Fig.2b, d**). Two months after SARS-CoV-  
177 2 virus has been cleared, *Aspergillus* (20.6%), *Trametes* (10.6%), *Yarrowia*  
178 (4.8%), and *Komagataella* (3.6%) in CG were even higher than that in HCG or  
179 PDG (**Fig.2a, b, c and d**). As bacterial microecology shown before, fungal  
180 microecology rarely returned to normal two months after the SARS-CoV-2 has  
181 been removed.

182 **The persist oropharyngeal viral dysbiosis:** *Rhinovirus A*, *Rhinovirus C* and  
183 *Human gamma herpesvirus 4* were the major viruses in oropharyngeal swabs  
184 from HCG. In addition to the greatly increase of SARS-CoV-2, Human *beta*  
185 *herpesvirus 7* also increased in oropharyngeal swabs from PDG than that in  
186 HCG, but *Rhinovirus A* and *Rhinovirus C* decreased significantly. Opportunistic  
187 viruses, including Human *gamma herpesvirus 4*, *Human alpha herpesvirus 1*

188 and *Porcine type C oncovirus* were richer in oropharyngeal swabs from CG than  
189 that in HCG and PDG(**Fig.3a**).

190 **Little changes in  $\alpha$ -diversity among HCG, PDG and CG:** We investigated  
191 longitudinal dynamics of oropharynx microbial (include bacteria and fungi)  
192 profiles in COVID-19 over time of exacerbation and explored whether recovery  
193 from *SARS-CoV-2* infection was associated with restoration of oropharyngeal  
194 microbial profiles to a community similar to that of healthy individuals. Results  
195 from  $\alpha$ -diversity microbial analyses (measured by the Shannon Diversity Index  
196 and Observed Diversity Index) have demonstrated little changes in  $\alpha$ -diversity  
197 among PDG, CG and HCG ( $P > 0.05$ ) (**Fig.4a, b**).

198 **Obviously changes in  $\beta$ -diversity among HCG, PDG and CG:** Principal  
199 coordinates analysis (PCoA) based on Bray-Curtis distance was used to  
200 visualize the apparent differences in microbial community structure. **Fig. 4c**  
201 shows that the PDG and CG are extremely separate from HCG, suggesting that  
202 oropharyngeal microbial structures were modulated by *SARS-CoV-2* infection  
203 and could not recover even virus was cleared two month later. The analysis of  
204 similarities (ANOSIM) plot shows that the inter-group difference was greater  
205 than the intra-group difference (**Fig. 4d**,  $R = 0.246$ ,  $P = 0.001$ ).

206 In conclusion, the *SARS-CoV-2* infection has a strong influence on the  
207 composition of oropharyngeal microbiome.

208 **Obviously changes in antibiotic resistance gene expression among HCG,**  
209 **PDG and CG:** To characterize antibiotic resistance gene expression profiles,

210 we analyzed the metatranscriptomic sequence reads based on Comprehensive  
211 Antibiotic Resistance Database (CARD 2020; <https://card.mcmaster.ca>).  
212 Across the dataset, we identified genes that confer resistance to 13 classes of  
213 antibiotics (**Fig. 5a, b**) with variations across the swabs. The expression of  
214 multidrug resistance genes (especially multidrug resistance, *tetracycline* and  
215 *glycopeptide*) in the oropharyngeal microbiome of patients with COVID-19 were  
216 higher than that in healthy controls, and returned to normal two months after  
217 virus clearance.

#### 218 **Alteration of main oropharyngeal microbial composition reflects disease** 219 **severity of patients with COVID-19**

220 In order to explore the role of oropharyngeal microbiome in patients with  
221 COVID-19, PDG subjects were further categorized as mild, moderate, severe,  
222 and critical according to the Diagnosis and Treatment Scheme for COVID-19  
223 released by the National Health Commission of China (Version7)[8, 13, 14], and  
224 mild, moderate patients with COVID-19 were divided as mild-moderate group  
225 (MMG), severe and critical patients with COVID-19 were divided as severe-  
226 critical group (SCG). Associations between alteration of main oropharyngeal  
227 microbial composition in patients with COVID-19 and the magnitude of COVID-  
228 19 severity were analysed.

229 ***Prevotella* increased gradually along with the symptom aggravated:** Top20  
230 Notably, *Prevotella* increased significantly in PDG than that in HCG (Wilcoxon  
231 rank-sum test,  $p < 0.001$ ) ( **Fig.1d**). As to the subgroup of PDG, Top20 bacterial

232 profiles in oropharyngeal swabs from MMG and SCG were shown as **Fig.6a, b**.  
233 The abundance of *Prevotella* in SCG was significantly higher (20.1%) than that  
234 in MMG (17.3%) (**Fig.6c**). *Prevotella* increased gradually, along with the  
235 severity of patients with COVID-19 aggravated gradually. (**Fig.6d**). To  
236 investigate the potential effects of the *Prevotella* in oropharynx of patients with  
237 COVID-19, we used a spearman analysis strategy for the parallel evaluation of  
238 all quantitative clinical traits from COVID-19 patients. Remarkably, there was  
239 a positive correlation between *Prevotella* and the elevation of Neutrophil  
240 percentage ( $R = 0.301$ ,  $p = 0.040$ ) (**Fig.6e**). These results indicated that it would  
241 be necessary to verify the synergic role of *Prevotella* in inducing severity of  
242 SARS-CoV-2 mediated pneumonia.

243 ***Aspergillus* increased remarkably in critical Patients with COVID-19:** It  
244 was observed that patients with severe COVID-19 had an increased risk of  
245 coexisting *Aspergillus* infection [18]. As to the subgroup of PDG, Top20 fungal  
246 profiles in oropharyngeal swabs specimens from MMG and SCG were shown  
247 as **Fig.7a, b**. The abundance of *Aspergillus* in SCG was significantly higher  
248 (21.7%) than that in MMG (19.8%) (**Fig.7c**). In particularly, *Aspergillus*  
249 increased remarkably in critical Patients with COVID-19 (**Fig.7d**). Therefore,  
250 monitoring the change in abundance of *Aspergillus* in oropharynx of COVID-19  
251 patients should be considered[18, 19].

252 **Decreased  $\alpha$ -diversity appeared to be associated with COVID-19 severity:**

253 The  $\alpha$ -diversity of oropharyngeal microbial profiles did not differ between

254 healthy controls and patients with COVID-19 (**Fig. 4a,b**,  $P > 0.05$ ). However, the  
255 diversity and richness of oropharyngeal microbial profiles were both  
256 significantly lower in SCG group than MMG group. Obviously, the  $\alpha$ -diversity  
257 decreased gradually along with the symptom aggravated(**Fig. 8a,b**,  $P < 0.01$ ).  
258 Besides, Principal coordinates analysis (PCoA) of  $\beta$ -diversity between SCG  
259 and MMG demonstrated that the microbial cluster away from each other  
260 (**Fig.8c**), there were also significant differences among mild, moderate, severe,  
261 and critical groups (**Fig.8d**).

262 **The severity of COVID-19 was positively correlated with higher SARS-**  
263 **CoV-2 viral load: Fig.3b and Fig.3c** showed that severe and critical patients  
264 with COVID-19 had much higher SARS-CoV-2 viral load than others. There was  
265 a negative correlation between SARS-CoV-2 viral load and platelet counts ( $R =$   
266  $-0.330$ ,  $P = 0.022$ ) (**Fig.3d**). These results indicated that SARS-CoV-2 viral load  
267 may be a biomarker to evaluate if they are able to predict lower platelet counts  
268 and correlate with the severity of COVID-19 disease. In conclusion, early check  
269 of SARS-CoV-2 viral load by metatranscriptome may be helpful for early  
270 detection of critically COVID-19 patients.

## 271 **Discussion**

272 SARS-COV-2 and other viral infections may alter the microbial composition of  
273 the upper respiratory tract, foster enhanced growth of pathogens, and facilitate  
274 the subsequent entry of large microbial loads into the lower respiratory tract [8,  
275 12, 20, 21], which are frequently associated with a more severe clinical

276 course[12, 18, 19, 22-24]. Besides, a specific bacterial formulation has showed  
277 a significant ameliorating impact on the clinical conditions of patients positive  
278 for *SARS-CoV-2* infection[25]. And given the unequivocal association between  
279 gut microbiota composition and COVID-19 disease severity, there is a pressing  
280 need to better understand how perturbation of the host oropharyngeal  
281 microbiome correlates with *SARS-COV-2* infections[6]. Based on analysis  
282 unbiased metatranscriptomic data, our longitudinal study has firstly confirmed  
283 that oropharyngeal microbiome composition reflects disease severity and  
284 presents long-term dysbiosis in patients with COVID-19.

285 The bacterial and fungal microecology of oropharynx were significantly  
286 perturbed by *SARS-CoV-2* infection, and they were even hard to return back to  
287 normal two months after the virus was cleared. Certainly, it is hard to ignore the  
288 influence of antibiotic exposure on URT microbiome. However, recent proof  
289 demonstrated that antibiotic drugs have short-term influence on the human gut  
290 microbiome with the bacterial community largely recovering within 30 days of  
291 antibiotic treatment[26, 27]. So, we speculate that *SARS-COV-2* infection is the  
292 key factor affecting the microecological dynamics of oropharynx. As other viral  
293 infections, antiviral immune responses induced by *SARS-COV-2* is associated  
294 with changes in microbial composition and function in the URT, which in turn  
295 may alter immune function of URT, thereby enhancing the sustainable  
296 proliferation of some bacterial species[12, 21].

297 Our study conducted in healthy subjects and who underwent *SARS-COV-2*

298 infection failed to demonstrate obvious changes in  $\alpha$ -diversity of the  
299 oropharyngeal microbiome. Thus, as other viral infections[12], the effects of  
300 *SARS-COV-2* infection on diversity itself are not presently considered a good  
301 indicator of risk for complications, including secondary bacterial pneumonias.  
302 The effect of *SARS-COV-2* infection on  $\alpha$  diversity is variable and is not  
303 currently considered a good indicator of the viral infection. Nevertheless, our  
304 study in patients with *SARS-COV-2* demonstrated that the  $\alpha$ -diversity of  
305 oropharyngeal microbiome decreased significantly associated with COVID-19  
306 severity.

307 In recent studies by next generation sequencing and MinION sequencing,  
308 *Prevotella* was found to be the common bacteria in URT of patients with COVID-  
309 19 [28, 29]. Notably, rich *Prevotella* was also detected in the intestines of  
310 patients with COVID-19[3]. The synergism of *Prevotella* in causing the severity  
311 of streptococcus pneumoniae mediated pneumonia was already known[30].  
312 Our data about patients with COVID-19 further demonstrated that *Prevotella* in  
313 oropharynx increased gradually consist with the symptom aggravated and  
314 could not return back to normal even two months after the *SARS-COV-2* was  
315 cleared. Through microaspiration from URT, *Prevotella* could participate in the  
316 immune homeostasis of the low respiratory tract [31], and pulmonary  
317 inflammation had been associated with accumulation of the pulmonary  
318 microbiome with *Prevotella*, this bacterium mainly activated Toll-like receptor 2  
319 and enhanced the expression IL-23 and IL-1 [32]. In vitro, *Prevotella* could

320 stimulate the production of IL-8, IL-6, and CCL20 in lung epithelial cells, which  
321 promoted neutrophil recruitment [33]. In vivo, we also confirmed that there was  
322 a positive correlation between *Prevotella* and the elevation of Neutrophil  
323 percentage. Latest evidence about host-pathogen interactions in the severity of  
324 COVID-19 also confirmed *Prevotella* proteins were over expressed in patients  
325 with COVID-19, and *Prevotella* proteins, but not SARS-COV-2 proteins were  
326 involved in multiple interactions with NF-kB, which was involved in increasing  
327 clinical severity of COVID-19[34]. In conclusion, *Prevotella* may play an  
328 important role in COVID-19 outbreak and should be given attention for  
329 understanding disease mechanisms and improving treatment outcomes.

330 *Aspergillus* is a common fungal pathogen of secondary infection in patients with  
331 critical COVID-19[18, 19, 35, 36]. Our results showed that *Aspergillus* increased  
332 remarkably in oropharynx of critical Patients with COVID-19. The respiratory  
333 tract is an interconnected system consisting of oropharynx and low respiratory  
334 tract, with microaspiration serving as the primary route of *Aspergillus*  
335 immigration from the oropharynx to the low respiratory tract. Therefore, for early  
336 detection of secondary fungal infections, monitoring the change in abundance  
337 of *Aspergillus* in oropharynx of patients with COVID-19 should be considered.

338 Soon after the onset of the global SARS-CoV-2 epidemic, the presence of other  
339 common respiratory viruses declined and even disappeared[22, 28]. Our  
340 results by metatranscriptomics are consistent with the absence of other  
341 common respiratory virus coinfection in patients with COVID-19. More

342 importantly, the severity of COVID-19 was positively correlated with higher  
343 *SARS-CoV-2* viral load and opportunistic viruses were rich even fully recovered  
344 two months later, and there was a negative correlation between *SARS-CoV-2*  
345 viral load and platelet counts. Platelet count showed significantly lower levels  
346 in severe patients compared to non-severe patients[37]. Meta-analysis of 1799  
347 patients also revealed those with severe COVID-19 infections had significantly  
348 lower platelet counts [37, 38].Therefore, besides keeping an eye on  
349 opportunistic viral infection of convalescent patients with COVID-19, early  
350 check of *SARS-CoV-2* viral load by metatranscriptome may be helpful for early  
351 detection of critically COVID-19 patients.

352 More importantly, we firstly performed metatranscriptomics to characterize the  
353 abundance and diversity of antibiotic resistance genes in the oropharynx  
354 microbiome of patients with COVID-19. Higher relative abundance of antibiotic  
355 resistance genes in the oropharyngeal microbiome of patients with COVID-19  
356 were decreased to normal two months after virus clearance. In line with  
357 previous study[26], Characterization of bacterial antibiotic resistance genes in  
358 the URT microbiome of patients with COVID-19 might help better to choose the  
359 appropriate antibiotics for bacterial co-infection and secondary infection in  
360 patients with COVID-19.

## 361 **Conclusions**

362 *SARS-CoV-2* primarily infects the respiratory tract and significantly perturbs  
363 microecology of oropharynx. Alterations in oropharyngeal microbial

364 composition, particularly of *Prevotella* and *Aspergillus*, reflect the severity of  
365 disease in patients with COVID-19. Furthermore, the oropharyngeal  
366 microbiome in patients with COVID-19 present persistent dysbiosis two months  
367 after clearance of the SARS-CoV-2 virus. These findings underscore an urgent  
368 need to understand the specific roles of oropharyngeal microorganisms in  
369 COVID-19 disease progression and rehabilitation as well as co-infection and  
370 secondary infection.

### 371 **Abbreviations**

372 SARS-CoV-2: severe acute respiratory syndrome coronavirus 2

373 COVID-19: coronavirus disease 2019

374 URT: upper respiratory tract

375 PDG: period of disease group

376 CG: convalescent group

377 HCG: healthy controls group

378 RT-qPCR: quantitative reverse transcription polymerase chain reaction

### 379 **Methods**

#### 380 **Study design and specimens collect**

381 We recruited 47 patients with COVID-19 confirmed by positive SARS-CoV-2  
382 quantitative reverse transcription PCR(RT-qPCR) to establish a longitudinal  
383 cohort study. The severity status of confirmed COVID-19 cases was  
384 categorized as mild, moderate, severe, and critical according to the Diagnosis  
385 and Treatment Scheme for COVID-19 released by the National Health

386 Commission of China (Version 7). As healthy controls group, we recruited 40  
387 healthy human subjects free of any respiratory infections during the same  
388 timeframe. Written consents were obtained from patients or their guardian(s).  
389 Clinical information and demographic information were collected.  
390 Oropharyngeal samples were obtained for routine diagnostic purposes, and the  
391 residual clinical diagnostic samples were provided for research and  
392 surveillance purposes. We collected oropharyngeal swabs at two time points  
393 (Within a week of diagnosis COVID-19 and two months after clearance of the  
394 SARS-CoV-2 virus. During the same timeframe, we collected oropharyngeal  
395 swabs from 40 healthy human subjects free of any respiratory infections. In  
396 order to remove possible contamination, blank control samples, including  
397 another 6 swabs not sampled, were collected. After collection, the samples  
398 were placed into a tube containing 2mL viral RNA preservation solution.

#### 399 **Samples processing and quantitative real-time PCR test for COVID-19**

400 Total RNA was extracted using QIAamp viral RNA mini kit (QIAGEN 52904,  
401 Germany) following the manufacturer's protocol.

402 Real-time RT-PCR was performed by amplifying two target genes, including  
403 open reading frame 1ab (ORF1ab) and nucleocapsid protein (N) using RT-PCR  
404 kit (Sansure Biotech Inc, China) on a Real-time PCR thermal cycler (ABI 7500  
405 system, Applied Biosystems instruments, USA).

#### 406 **Metatranscriptomic sequencing**

407 After extraction, the first strand cDNA was prepared by priming with random

408 hexamers followed. Standard RNAseq library was constructed using NGS  
409 library construction kit (Genskey 1906). The libraries were sequenced on  
410 Illumina NextSeq 500-sequencer using a 75-cycle single-end sequencing  
411 strategy and each sample will get nearly 20 million reads.

#### 412 **Data processing**

413 First, software fastp (parameters: -q 15 -u 40 -l 50, version: 0.19.5) [39] was  
414 used to filter low-quality reads, remove adapter and Komplexity (parameters: -  
415 t 0.4, version: Nov-2019)[40]was used to remove low complexity reads for raw  
416 data. Then, filtered reads were mapped to the ensembl 84 (GRCh38) human  
417 reference genome to remove host sequences using HISAT2 (version 2.1.0) with  
418 default parameters [41]. Next, unmapped reads were annotated taxonomic  
419 classifications by Kraken2 (version 2.0.9, parameters: --threads 24 --  
420 confidence 0.1)[42]with a self-build database (built by downloading all the  
421 complete genomes from NCBI Refseq database, including the SARS-COV-2  
422 reference NC\_045512.2. And only genomes from archaea, bacteria, fungi,  
423 protozoa and viral were selected for building a classification database for  
424 Kraken2 (k=35, l=31)). Then, abundance of taxonomy was estimated using  
425 Bracken (version 2.5, parameters: -r 75 -l G, S -t 0) [43]. Finally, microorganisms  
426 satisfying the following criteria were retained for the subsequent analysis: (1)  
427 archaea, bacteria, fungi, or virus; (2) 10-fold higher filtered RPM than that in the  
428 negative control (NC); (3) no batch effect; (4) no known contamination;(5) only  
429 human virus.

430 In order to obtain information of antibiotic resistance gene. First, unmapped  
431 reads were assembled using SPAdes (version: 3.13.0) with default parameters  
432 [44] and scaffolds less than 150 bp were removed. Then, MetaGeneMark [45]  
433 was used to predict protein coding genes from the above filtered scaffolds. Next,  
434 the abundance of antibiotic resistance genes were annotated by aligning the  
435 sequence of the above predicted genes to Comprehensive Antibiotic  
436 Resistance Database (CARD 2020; <https://card.mcmaster.ca>) [46] using the  
437 HISAT2 alignment method with default parameters. Each gene was filtered to  
438 have at least two matching reads. Finally, only antibiotic resistance genes  
439 occurred in >25% of samples were used for further statistical analyses.

#### 440 **Statistical analysis**

441 Statistical analyses were done using R (version 3.5.1). The  $\alpha$ -diversity was  
442 analyzed by vegan function with R packages. Principal co-ordinates analysis  
443 (PCoA) was based on Bray-Curtis dissimilarity (BCD) distance matrices [47].  
444 Differences between groups in the  $\alpha$ -diversity were evaluated using the Mann-  
445 Whitney test or the Kruskal-Wallis test. False discovery rate (FDR) values were  
446 estimated using the Benjamini–Yekutieli method to control for multiple testing  
447 [48]. Principal component analysis (PCA) was analyzed by prcomp function with  
448 R packages [49]. Analysis of similarities (ANOSIM) was used to statistically test  
449 whether there is a significant difference between two or more groups of  
450 sampling units [50]. The log<sub>10</sub> value was used to show the abundance of  
451 antibiotic resistance gene. Finally, the spearman correlation method [51] was

452 used to analyze the correlation analysis between microbe and clinical index,  
453 and a correlation coefficient of more than 0.300 is considered [52]. A p-value of  
454 < 0.05 was considered statistically significant. Concerning symbols used to  
455 represent higher orders of significance,  $P < 0.05$  was indicated by \*,  $P < 0.01$  by  
456 \*\* and  $P < 0.001$  by \*\*\*.

### 457 **Acknowledgements**

458 We thank Yannan Lini for assistance with processing language editing of the  
459 manuscript. We thank Genskey for their assistance in the sequencing work.

### 460 **Authors' contributions**

461 WML, BWY, DL, YZZ, MJL and MJW contributed substantially to the conception  
462 and design of the study and interpretation and wrote the manuscript. RQ, TBD,  
463 LJ, JZ and YLL undertook clinical sample collection and processing and  
464 analyses of clinical records. YZZ, SFL, MJL, MJW, JMM, YCM, ZYZ, JMM and  
465 JX contributed substantially to the acquisition of data and the analysis. YZZ and  
466 SFL contributed substantially to data interpretation. The authors read and  
467 approved the final manuscript.

### 468 **Funding**

469 This work was funded by the Sichuan Provincial Program for Diagnostic and  
470 Treatment of COVID-19 (2020YFS0002, 2020YFS0001, 2020YFS0572).

### 471 **Availability of data and materials**

472 The sequencing data from this study have been deposited in the CNSA ([https://  
473 db.cngb.org/cnsa/](https://db.cngb.org/cnsa/)) of CNGBdb with accession number CNP0001393.

474 **Ethics approval and consent to participate**

475 This study was approved by The Biomedical Research Ethics Committee of  
476 West China Hospital and the document IDs are NO.2020(100), NO.2020 (193)  
477 and NO.2020 (267). Written consents were obtained from patients or their  
478 guardian(s). All work was performed in accordance with the Helsinki  
479 Declaration.

480 **Consent for publication**

481 Not applicable.

482 **Competing interests**

483 The authors declare that they have not competing interests.

484 **References**

- 485 1. Zhu N, Zhang D, Wang W, Li X, Yang B, Song J, Zhao X, Huang B, Shi W, Lu R *et al*: **A Novel**  
486 **Coronavirus from Patients with Pneumonia in China, 2019.** *N Engl J Med* 2020, **382**(8):727-  
487 733.
- 488 2. Microbiome Centers Consortium CC: **Coordinating and Assisting Research at the SARS-CoV-**  
489 **2/Microbiome Nexus.** *mSystems* 2020, **5**(6).
- 490 3. Tao W, Wang X, Zhang G, Guo M, Ma H, Zhao D, Sun Y, He J, Liu L, Zhang K *et al*: **Re-detectable**  
491 **positive SARS-CoV-2 RNA tests in patients who recovered from COVID-19 with intestinal**  
492 **infection.** *Protein Cell* 2020.
- 493 4. Zuo T, Zhang F, Lui GCY, Yeoh YK, Li AYL, Zhan H, Wan Y, Chung ACK, Cheung CP, Chen N *et al*:  
494 **Alterations in Gut Microbiota of Patients With COVID-19 During Time of Hospitalization.**  
495 *Gastroenterology* 2020, **159**(3):944-955.e948.

- 496 5. Zuo T, Zhan H, Zhang F, Liu Q, Tso EYK, Lui GCY, Chen N, Li A, Lu W, Chan FKL *et al*: **Alterations**  
497 **in Fecal Fungal Microbiome of Patients With COVID-19 During Time of Hospitalization until**  
498 **Discharge.** *Gastroenterology* 2020, **159**(4):1302-1310 e1305.
- 499 6. Yeoh YK, Zuo T, Lui CY, Zhang F, Ng SC: **Gut microbiota composition reflects disease severity**  
500 **and dysfunctional immune responses in patients with COVID-19.** *Gut* 2021:gutjnl-2020-  
501 323020.
- 502 7. Chen Y, Gu S, Chen Y, Lu H, Shi D, Guo J, Wu WR, Yang Y, Li Y, Xu KJ *et al*: **Six-month follow-up**  
503 **of gut microbiota richness in patients with COVID-19.** *Gut* 2021.
- 504 8. Shen Z, Xiao Y, Kang L, Ma W, Shi L, Zhang L, Zhou Z, Yang J, Zhong J, Yang D *et al*: **Genomic**  
505 **Diversity of Severe Acute Respiratory Syndrome-Coronavirus 2 in Patients With Coronavirus**  
506 **Disease 2019.** *Clin Infect Dis* 2020, **71**(15):713-720.
- 507 9. Qin T, Geng T, Zhou H, Han Y, Ren H, Qiu Z, Nie X, Du T, Liang J, Du P *et al*: **Super-dominant**  
508 **pathobiontic bacteria in the nasopharyngeal microbiota as causative agents of secondary**  
509 **bacterial infection in influenza patients.** *Emerg Microbes Infect* 2020, **9**(1):605-615.
- 510 10. Martin-Loeches I, M JS, Vincent JL, Alvarez-Lerma F, Bos LD, Sole-Violan J, Torres A, Rodriguez  
511 **A: Increased incidence of co-infection in critically ill patients with influenza.** *Intensive Care*  
512 *Med* 2017, **43**(1):48-58.
- 513 11. Kaul D, Rathnasinghe R, Ferres M, Tan GS, Barrera A, Pickett BE, Methe BA, Das SR, Budnik I,  
514 Halpin RA *et al*: **Microbiome disturbance and resilience dynamics of the upper respiratory**  
515 **tract during influenza A virus infection.** *Nat Commun* 2020, **11**(1):2537.
- 516 12. Hanada S, Pirzadeh M, Carver KY, Deng JC: **Respiratory Viral Infection-Induced Microbiome**  
517 **Alterations and Secondary Bacterial Pneumonia.** *Front Immunol* 2018, **9**:2640.

- 518 13. Jian W, Jun L, Xinguo Z, Chengyuan L, Wei W, Dawei W, Wei X, Chunyu Z, Jiong Y, Bin J: **Clinical**  
519 **Characteristics of Imported Cases of Coronavirus Disease 2019 (COVID-19) in Jiangsu**  
520 **Province: A Multicenter Descriptive Study.** *Clinical Infectious Diseases*.
- 521 14. Lu J, du Plessis L, Liu Z, Hill V, Kang M, Lin H, Sun J, Francois S, Kraemer MUG, Faria NR *et al*:  
522 **Genomic Epidemiology of SARS-CoV-2 in Guangdong Province, China.** *Cell* 2020, **181**(5):997-  
523 1003 e1009.
- 524 15. Zhang H, Ai JW, Yang W, Zhou X, Zhang W: **Metatranscriptomic Characterization of COVID-19**  
525 **Identified A Host Transcriptional Classifier Associated With Immune Signaling.** *Clinical*  
526 *Infectious Diseases* 2020.
- 527 16. **The nasal cavity microbiota of healthy adults.** *Microbiome* 2014, **2**(1):1-5.
- 528 17. Lemon KP, Klepac-Ceraj V, Schiffer HK, Brodie EL, Lynch SV, Kolter R: **Comparative analyses of**  
529 **the bacterial microbiota of the human nostril and oropharynx.** *mBio* 2010, **1**(3).
- 530 18. Koehler P, Cornely OA, Bottiger BW, Dusse F, Eichenauer DA, Fuchs F, Hallek M, Jung N, Klein F,  
531 Persigehl T *et al*: **COVID-19 associated pulmonary aspergillosis.** *Mycoses* 2020, **63**(6):528-534.
- 532 19. Gangneux JP, Bougnoux ME, Dannaoui E, Cornet M, Zahar JR: **Invasive fungal diseases during**  
533 **COVID-19: We should be prepared.** *J Mycol Med* 2020, **30**(2):100971.
- 534 20. Wolter N, Tempia S, Cohen C, Madhi SA, Venter M, Moyes J, Walaza S, Malope-Kgokong B,  
535 Groome M, du Plessis M *et al*: **High nasopharyngeal pneumococcal density, increased by viral**  
536 **coinfection, is associated with invasive pneumococcal pneumonia.** *J Infect Dis* 2014,  
537 **210**(10):1649-1657.
- 538 21. Haocheng Z, Jing-Wen A, Wenjiao Y, Xian Z, Fusheng H, Shumei X, Weiqi Z, Yang L, Yiqi Y, Xuejing  
539 **G: Metatranscriptomic Characterization of COVID-19 Identified A Host Transcriptional**

540 **Classifier Associated With Immune Signaling.** *Clinical Infectious Diseases.*

541 22. Calcagno A, Ghisetti V, Burdino E, Trunfio M, Allice T, Boggione L, Bonora S, Di Perri G:

542 **Coinfection with other respiratory pathogens in COVID-19 patients.** *Clin Microbiol Infect* 2020.

543 23. Langford BJ, So M, Raybardhan S, Leung V, Westwood D, MacFadden DR, Soucy JR, Daneman

544 N: **Bacterial co-infection and secondary infection in patients with COVID-19: a living rapid**

545 **review and meta-analysis.** *Clin Microbiol Infect* 2020.

546 24. Kim D, Quinn J, Pinsky B, Shah NH, Brown I: **Rates of Co-infection Between SARS-CoV-2 and**

547 **Other Respiratory Pathogens.** *JAMA* 2020, **323**(20):2085-2086.

548 25. d'Ettorre G, Ceccarelli G, Marazzato M, Campagna G, Pinacchio C, Alessandri F, Ruberto F, Rossi

549 G, Celani L, Scagnolari C *et al*: **Challenges in the Management of SARS-CoV2 Infection: The**

550 **Role of Oral Bacteriotherapy as Complementary Therapeutic Strategy to Avoid the**

551 **Progression of COVID-19.** *Front Med (Lausanne)* 2020, **7**:389.

552 26. Seelbinder B, Chen J, Brunke S, Vazquez-Urbe R, Santhaman R, Meyer AC, de Oliveira Lino FS,

553 Chan KF, Loos D, Imamovic L *et al*: **Antibiotics create a shift from mutualism to competition in**

554 **human gut communities with a longer-lasting impact on fungi than bacteria.** *Microbiome*

555 2020, **8**(1):133.

556 27. MacPherson CW, Mathieu O, Tremblay J, Champagne J, Nantel A, Girard SA, Tompkins TA: **Gut**

557 **Bacterial Microbiota and its Resistome Rapidly Recover to Basal State Levels after Short-term**

558 **Amoxicillin-Clavulanic Acid Treatment in Healthy Adults.** *Sci Rep* 2018, **8**(1):11192.

559 28. Wang Z, Hu X, Li Z, Tu C, Wang Y, Pang P, Zhang H, Zheng X, Liang Y, Shan H *et al*: **Effect of SARS-**

560 **CoV-2 Infection on the Microbial Composition of Upper Airway.** *Infect Drug Resist* 2020,

561 **13**:2637-2640.

- 562 29. Moore SC, Penrice-Randal R, Alruwaili M, Randle N, Armstrong S, Hartley C, Haldenby S, Dong  
563 X, Alrezaihi A, Almsaud M *et al*: **Amplicon-Based Detection and Sequencing of SARS-CoV-2 in**  
564 **Nasopharyngeal Swabs from Patients With COVID-19 and Identification of Deletions in the**  
565 **Viral Genome That Encode Proteins Involved in Interferon Antagonism.** *Viruses* 2020, **12**(10).
- 566 30. Nagaoka K, Yanagihara K, Morinaga Y, Nakamura S, Harada T, Hasegawa H, Izumikawa K,  
567 Ishimatsu Y, Kakeya H, Nishimura M: **Prevotella intermedia Induces Severe Bacteremic**  
568 **Pneumococcal Pneumonia in Mice with Upregulated Platelet-Activating Factor Receptor**  
569 **Expression.** *Infection and Immunity* 2014, **82**(2):587-593.
- 570 31. Huffnagle GB, Dickson RP, Lukacs NW: **The respiratory tract microbiome and lung**  
571 **inflammation: a two-way street.** *Mucosal Immunol* 2017, **10**(2):299-306.
- 572 32. Segal LN, Alekseyenko AV, Clemente JC, Kulkarni R, Wu B, Chen H, Berger KI, Goldring RM, Rom  
573 WN, Blaser MJ: **Enrichment of lung microbiome with supraglottic taxa is associated with**  
574 **increased pulmonary inflammation.** *Microbiome* 2013, **1**.
- 575 33. Larsen, Madura J: **The immune response to Prevotella bacteria in chronic inflammatory**  
576 **disease.** *Immunology* 2017, **151**(4).
- 577 34. Khan AA, Khan Z: **COVID-2019-associated overexpressed Prevotella proteins mediated host-**  
578 **pathogen interactions and their role in coronavirus outbreak.** *Bioinformatics* 2020,  
579 **36**(13):4065-4069.
- 580 35. Vaillancourt M, Jorth P: **The Unrecognized Threat of Secondary Bacterial Infections with**  
581 **COVID-19.** *mBio* 2020, **11**(4).
- 582 36. Biesen SV, Kwa D, Bosman RJ, Juffermans NP: **Detection of Invasive Pulmonary Aspergillosis**  
583 **in COVID-19 with Non-directed Bronchoalveolar Lavage.** *American Journal of Respiratory and*

584 *Critical Care Medicine* 2020.

585 37. Kermali M, Khalsa RK, Pillai K, Ismail Z, Harky A: **The role of biomarkers in diagnosis of COVID-**

586 **19 - A systematic review.** *Life Sci* 2020, **254**:117788.

587 38. Lippi G, Plebani M, Henry BM: **Thrombocytopenia is associated with severe coronavirus**

588 **disease 2019 (COVID-19) infections: A meta-analysis.** *Clinica Chimica Acta* 2020.

589 39. Chen S, Zhou Y, Chen Y, Gu J: **fastp: an ultra-fast all-in-one FASTQ preprocessor.** *Bioinformatics*

590 2018, **34**(17):i884-i890.

591 40. Zijie S, Yan X, Lu K, Wentai M, Leisheng S, Li Z, Zhuo Z, Jing Y, Jiaxin Z, Donghong Y: **Genomic**

592 **Diversity of Severe Acute Respiratory Syndrome–Coronavirus 2 in Patients With Coronavirus**

593 **Disease 2019.** *Clinical Infectious Diseases.*

594 41. Kim D, Langmead B, Salzberg SL: **HISAT: A fast spliced aligner with low memory requirements.**

595 *Nature Methods* 2015, **12**(4).

596 42. Wood DE, Lu J, Langmead B: **Improved metagenomic analysis with Kraken 2.** *Genome biology*

597 2019, **20**(1).

598 43. Lu J, Breitwieser FP, Thielen P, Salzberg SL: **Bracken: estimating species abundance in**

599 **metagenomics data.** *Peerj Computer Science* 2017, **3**(1):e104.

600 44. Bankevich A, Nurk S, Antipov D, Gurevich AA, Dvorkin M, Kulikov AS, Lesin VM, Nikolenko SI,

601 Pham S, Prjibelski AD: **SPAdes: a new genome assembly algorithm and its applications to**

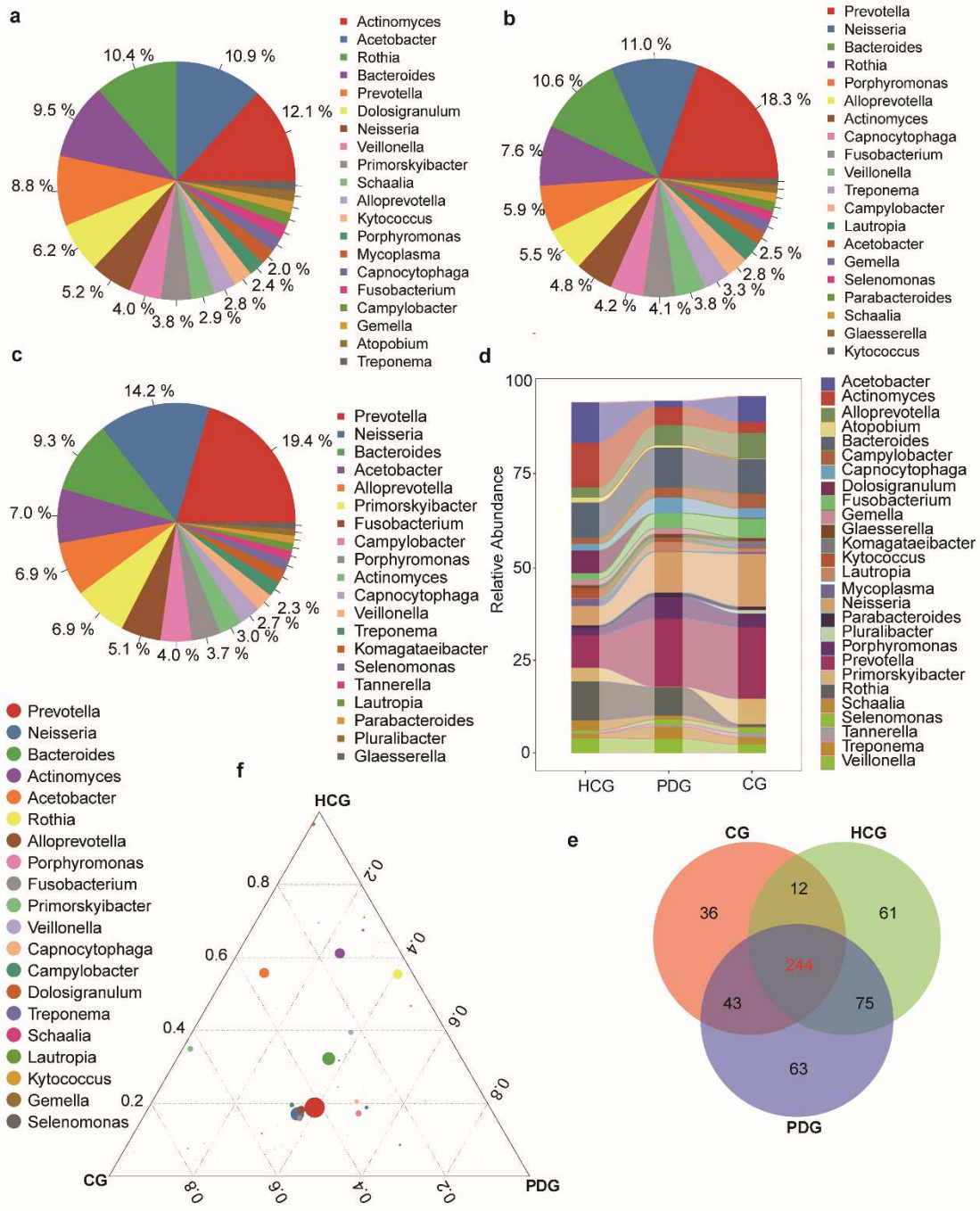
602 **single-cell sequencing.** *Journal of Computational Biology* 2012, **19**(5):455-477.

603 45. Wenhan Z, Alexandre L, Mark B: **Ab initio gene identification in metagenomic sequences.**

604 *Nucleic Acids Research* 2010, **38**(12):e132.

605 46. Alcock BP, Raphenya AR, Lau TTY, Tsang KK, Megane B, Arman E, William H, Nguyen A-LV, Cheng

- 606 AA, Sihan L: **CARD 2020: antibiotic resistome surveillance with the comprehensive antibiotic**  
607 **resistance database.** *Nucleic Acids Research.*
- 608 47. Kristi B, Brett WM, Sharon WT, Martin M, Mia J, Melissa Z, Taylor MW, Douglas RG:  
609 **Differentially Regulated Host Proteins Associated with Chronic Rhinosinusitis Are Correlated**  
610 **with the Sinonasal Microbiome.** *Frontiers in Cellular and Infection Microbiology* 2017, **7**:504-.
- 611 48. Benjamini Y, Yekutieli D: **The control of the false discovery rate in multiple testing under**  
612 **dependency.** *Annals of Statistics* 2001, **29**(4).
- 613 49. Dubey G, Kollah B, Gour VK, Shukla AK, Mohanty SR: **Diversity of bacteria and archaea in the**  
614 **rhizosphere of bioenergy crop *Jatropha curcas*.** *Biotech* 2016, **6**(2):257.
- 615 50. Marti, J., Anderson, Daniel, C., I., Walsh: **PERMANOVA, ANOSIM, and the Mantel test in the**  
616 **face of heterogeneous dispersions: What null hypothesis are you testing?** *Ecological*  
617 *Monographs* 2013.
- 618 51. De Winter JCF, Gosling SD, Potter J: **Comparing the Pearson and Spearman Correlation**  
619 **Coefficients Across Distributions and Sample Sizes: A Tutorial Using Simulations and**  
620 **Empirical Data.** *Psychological Methods* 2016, **21**(3):273-290.
- 621 52. Mukaka M: **Statistics corner: A guide to appropriate use of correlation coefficient in medical**  
622 **research.** *Malawi Medical Journal* 2012, **24**(3):69-71.



623

624 **Fig.1 Oropharyngeal bacterial characterization and alterations among HCG,**

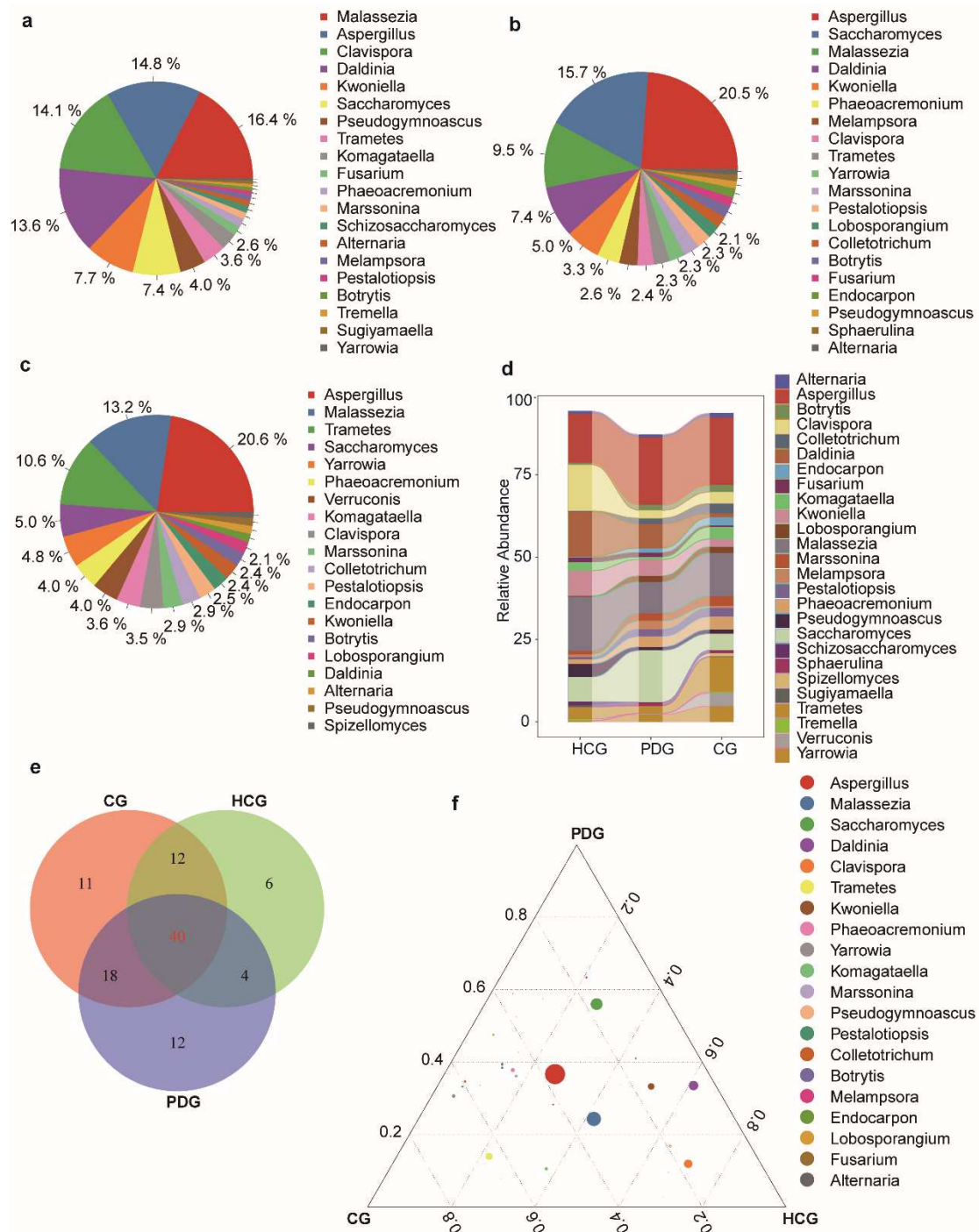
625 **PDG and CG. Average compositions of relative abundance of the top20**

626 **bacterial communities for each group at the genus level, a for HCG, b for PDG**

627 **and c for CG. d Alterations of top20 bacterial communities among the three**

628 **groups at the genus level, Especially, *Prevotella* is significantly higher in PDG**

629 than that in HCG (Wilcoxon rank-sum test,  $p < 0.001$ ). e Venn diagram showing  
630 shared and unique genus of the three groups. f Ternary plots depicting the 244  
631 shared bacterial landscape on genus level among HCG, PDG and CG group.  
632 The sum of the proportion for one specific bacteria in the three groups was set  
633 as 1, and the proportion of one specific bacteria in each group is equal to its  
634 corresponding relative abundance divided by the relative abundance sum of  
635 this bacteria in the three groups. The size of the circles represents the relative  
636 abundance of the genus.



637

638 **Fig.2 Oropharyngeal fungal characterization and alterations among HCG, PDG**

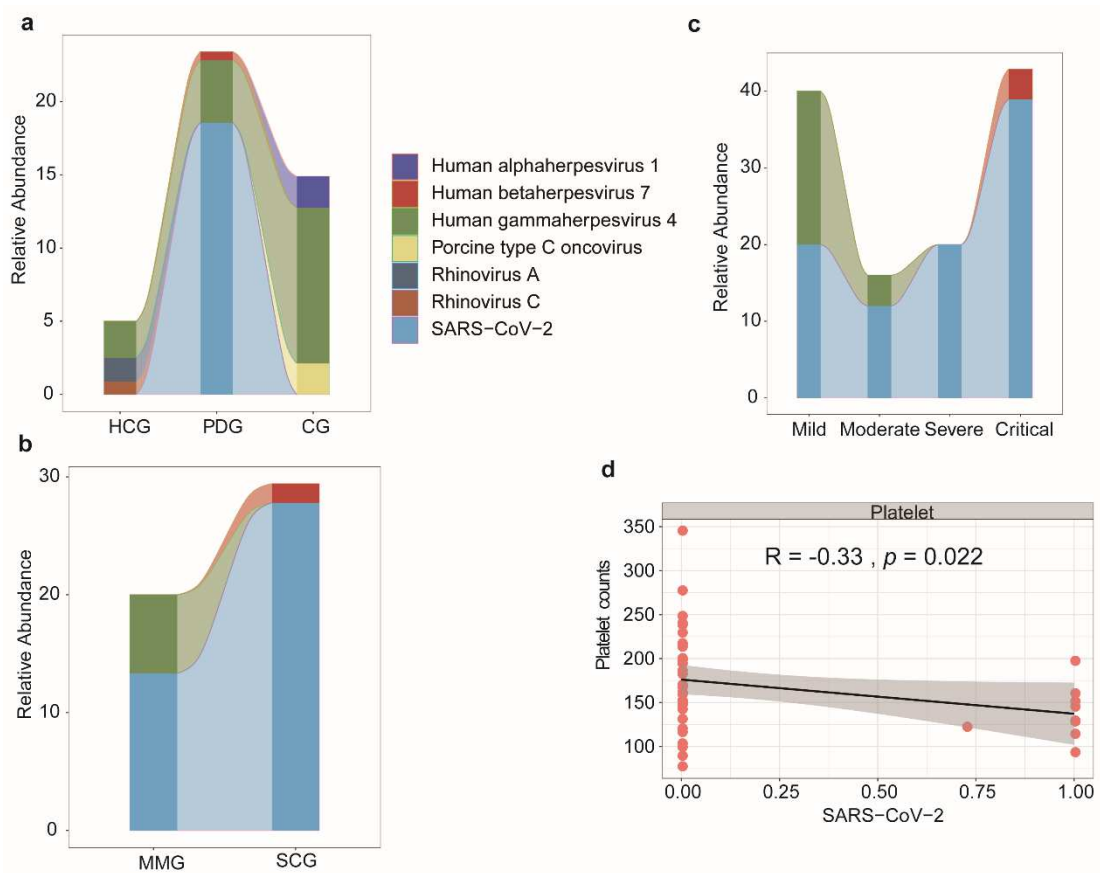
639 **and CG. Average compositions of relative abundance of the top20 fungal**

640 **communities for each group at the genus level, a for HCG, b for PDG and c for**

641 **CG. d Alterations of top20 fungal communities among the three groups at the**

642 **genus level. e Venn diagram showing shared and unique genus of the three**

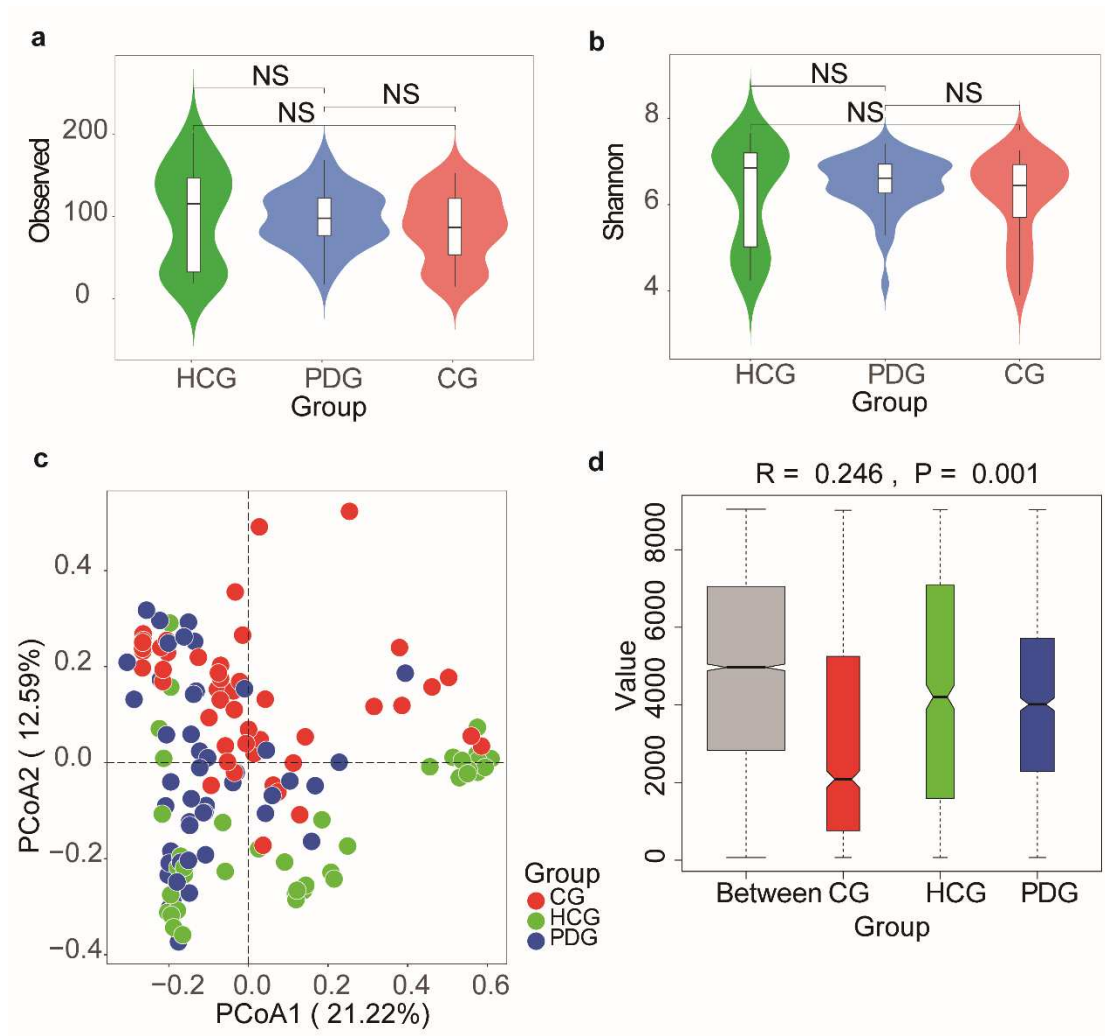
643 groups. f Ternary plots depicting the 244 shared fungal landscape on genus  
 644 level among HCG, PDG and CG group. The sum of the proportion for one  
 645 specific bacteria in the three groups was set as 1, and the proportion of one  
 646 specific fungi in each group is equal to its corresponding relative abundance  
 647 divided by the relative abundance sum of this fungi in the three groups. The  
 648 size of the circles represents the relative abundance of the genus.



649

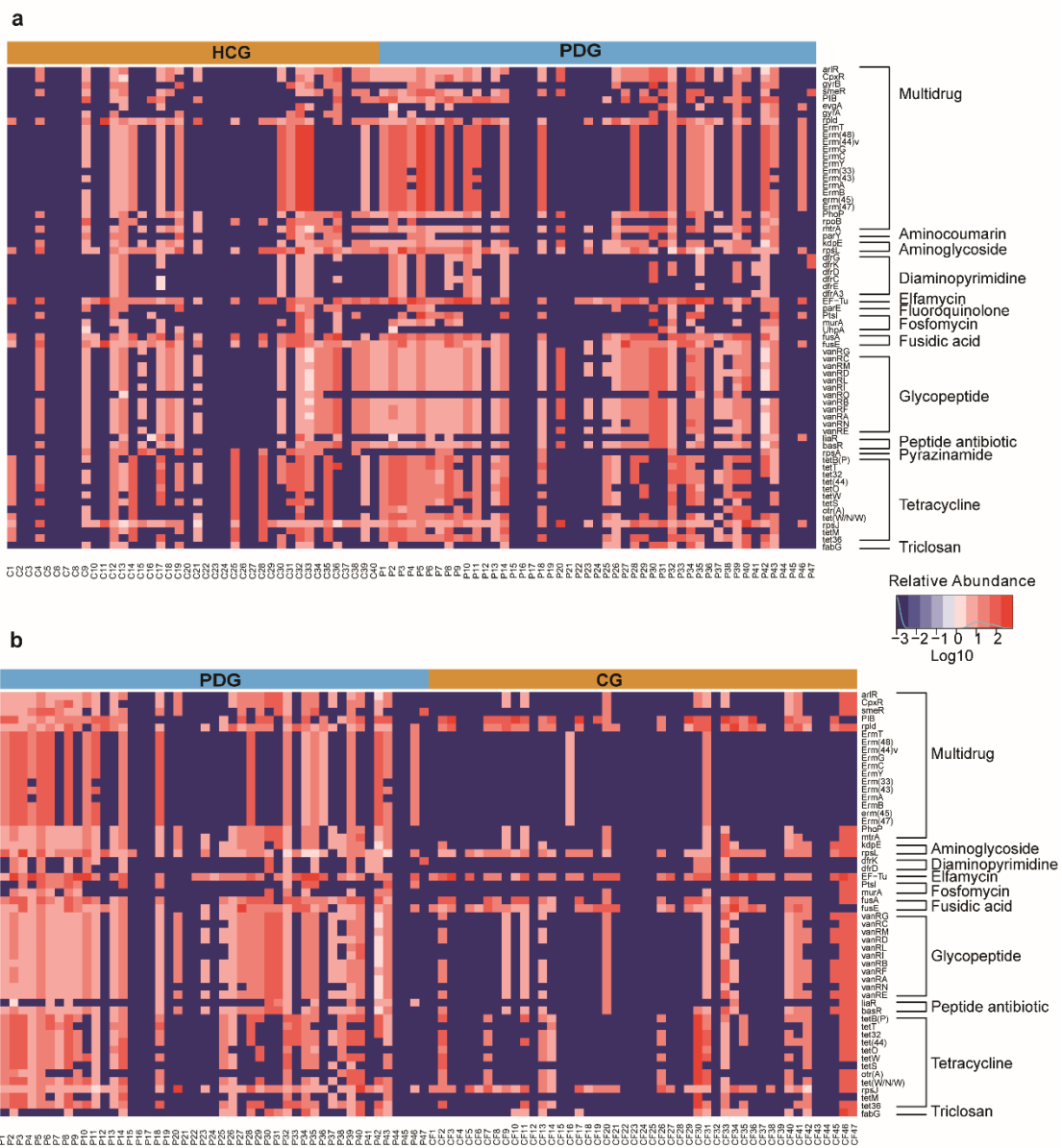
650 **Fig.3 Oropharyngeal *SARS-CoV-2* viral load was positively correlated with the**  
 651 **severity of COVID-19. a** The relative abundance changes of 7 oropharyngeal  
 652 viral species (including SARS-COR-2) among HCG, PDG and CG group, b  
 653 among MMG and SCG group, c among Mild, Moderate, Severe and Critical  
 654 group. d Negative correlation between *SARS-CoV-2* viral load (x-axis) and

655 platelet counts (y-axis) (Spearman correlation analysis:  $R = -0.330$ ,  $P = 0.022$ ),  
 656 Linear regression lines are shown in each scatter plot in black, and shaded  
 657 regions represent 95% confidence intervals.



658  
 659 **Fig.4 Oropharynx microbial alterations in diversity among HCG, PDG and CG.**  
 660 **a** Little changes in Observed index among HCG, PDG and CG (NS:  $P > 0.05$ ).  
 661 **b** Little changes in Shannon index among HCG, PDG and CG (NS:  $P > 0.05$ ). **c**  
 662 Principal coordinate analysis (PCoA) of Bray–Curtis distance showed obviously  
 663 changes in  $\beta$ -diversity among HCG, PDG and CG. The colors represent three  
 664 different groups. PCoA1 and PCoA2 represent the top two principal coordinates  
 665 that captured most of the diversity. The fraction of diversity captured by the

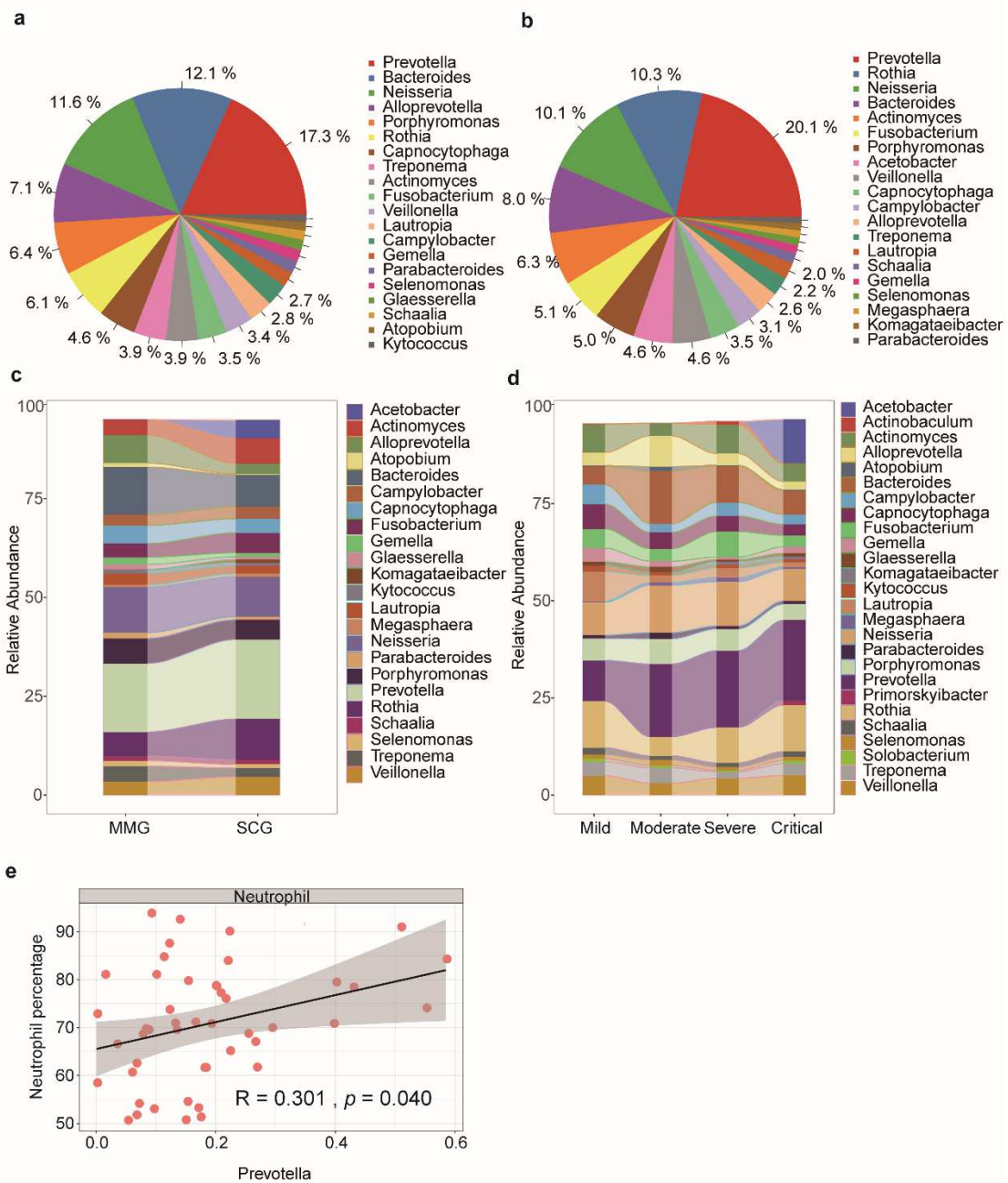
666 coordinate is valued as a percentage. **d.** The analysis of similarities (ANOSIM)  
 667 based on Bray–Curtis distance shows that  $R > 0$  and  $P < 0.05$ , indicating that  
 668 the inter-group difference among HCG, PDG and CG was greater than the intra-  
 669 group difference in each group. The R means the statistical value of ANOSIM,  
 670 y-axis value means Bray–Curtis rank, and 999 was used for the permutations.  
 671 NS means no significant.



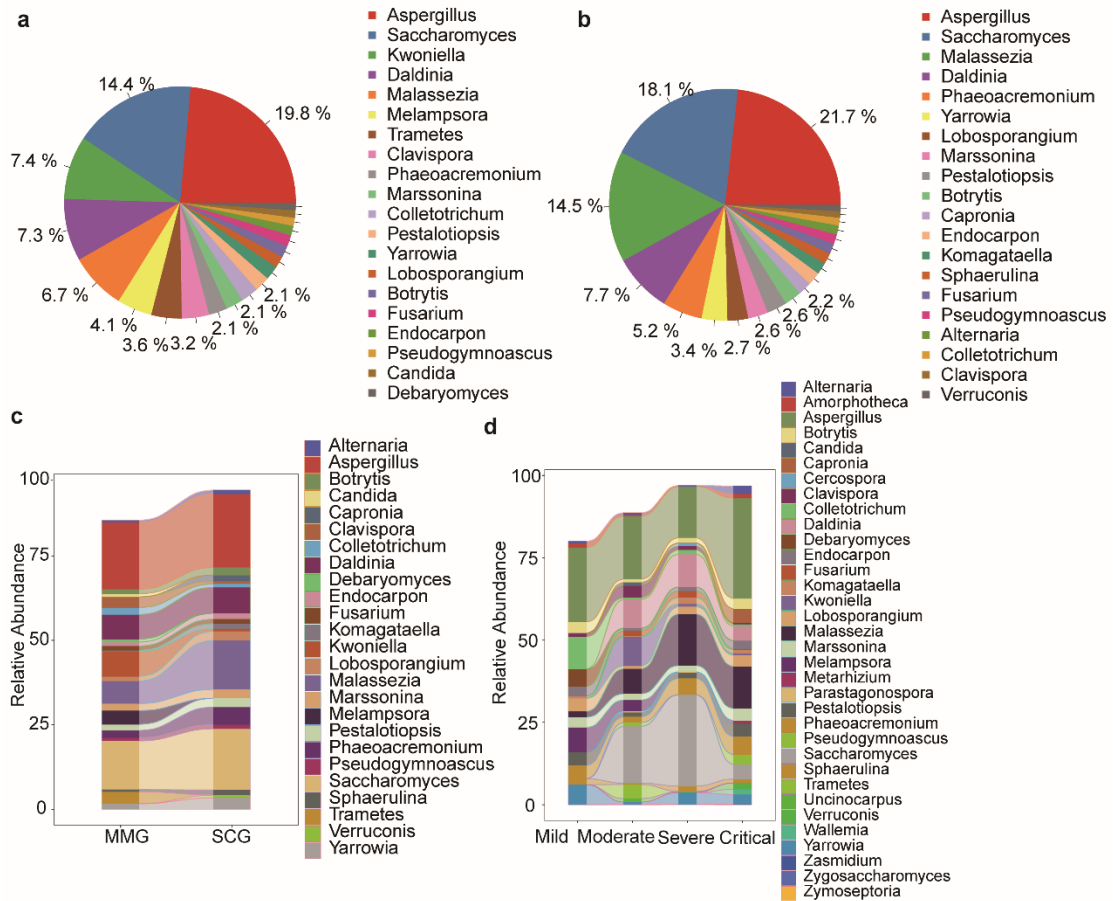
672

673 **Fig.5** Obviously changes of oropharynx microbial antibiotic resistance genes

674 expression among HCG, PDG and CG. a Heatmap for the relative abundances  
 675 of microbial antibiotic resistance genes expression between HCG and PDG. b  
 676 Heatmap for the relative abundances of microbial antibiotic resistance genes  
 677 expression between PDG and CG. The relative abundance changes from low  
 678 to high is showed by color changes from blue to red. The log10 value was used  
 679 to show the abundance of antibiotic resistance gene.



681 **Fig.6 Alterations of oropharyngeal bacteria reflected disease severity in**  
682 **patients with COVID-19. a, b** Average compositions of relative abundance of  
683 the top20 bacterial communities of MMG and SCG groups at the genus level. **c**  
684 Alterations of top20 bacterial communities among the MMG and SCG groups  
685 at the genus level. **d** Alterations of top20 bacterial communities among the Mild,  
686 Moderate, Severe and Critical groups at the genus level. Especially, the  
687 alteration of *Prevotella* gradually increased along with the symptom aggravated  
688 in patients with COVID-19. **e** Positive correlation between *Prevotella* relative  
689 abundance (x-axis) and the elevation of Neutrophil percentage (y-axis)  
690 (Spearman correlation analysis:  $R = 0.301$ ,  $p = 0.040$ ), Linear regression lines  
691 are shown in each scatter plot in black, and shaded regions represent 95%  
692 confidence intervals.



693

694 **Fig.7 Alterations of oropharyngeal fungi reflected disease severity in patients**

695 **with COVID-19. a, b Average compositions and relative abundance of the top20**

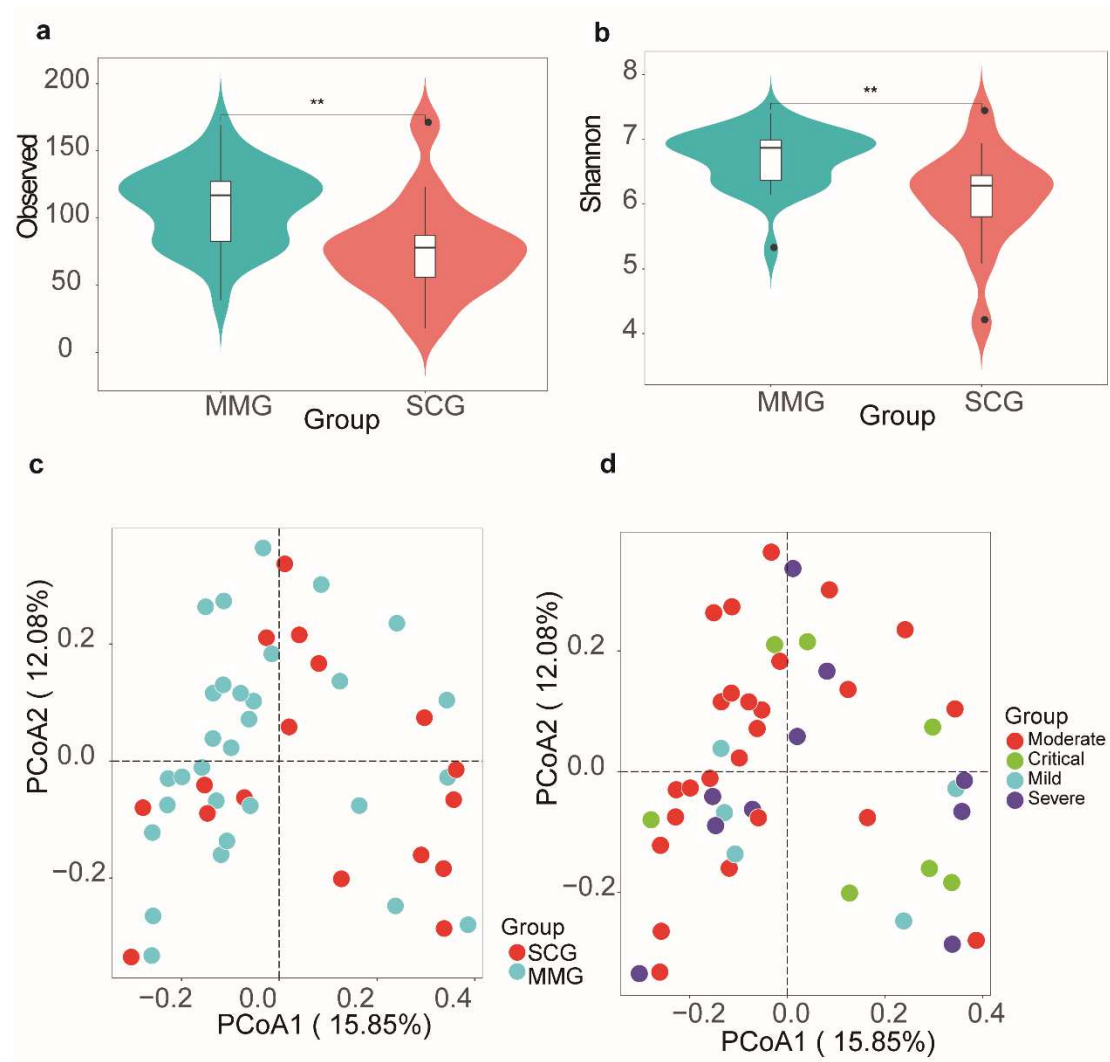
696 **fungal communities of MMG and SCG groups at the genus level. c Alterations**

697 **of top20 fungal communities among the MMG and SCG groups at the genus**

698 **level. d Alterations of top20 fungal communities among the Mild, Moderate,**

699 **Severe and Critical groups at the genus level. Especially, *Aspergillus* increased**

700 **remarkably in critical Patients with COVID-19.**



701

702 **Fig.8 Decreased oropharyngeal microbiome in diversity appeared to be**

703 **associated with COVID-19 severity. a Obviously decreased oropharyngeal**

704 **microbiome in Observed index between MMG and SCG (\*\*:  $P < 0.001$ ).**

705 **Obviously decreased oropharyngeal microbiome in Shannon index between**

706 **MMG and SCG (\*\*:  $P < 0.001$ ).** c Principal coordinate analysis (PCoA) of Bray–

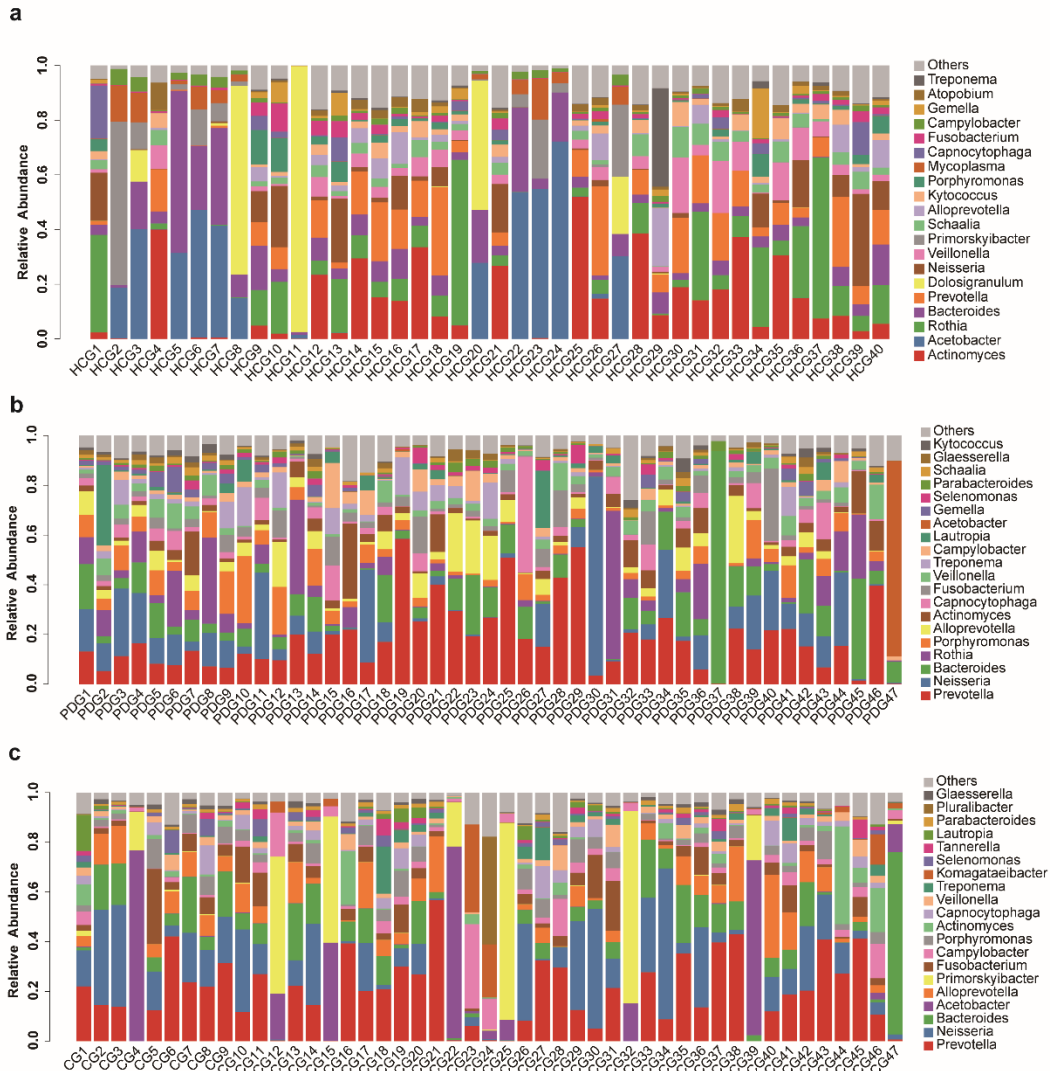
707 **Curtis distance showed obviously changes in  $\beta$ -diversity among MMG and SCG**

708 **groups. d Principal coordinate analysis (PCoA) of Bray–Curtis distance showed**

709 **obviously changes in  $\beta$ -diversity among Mild, Moderate, Severe and Critical**

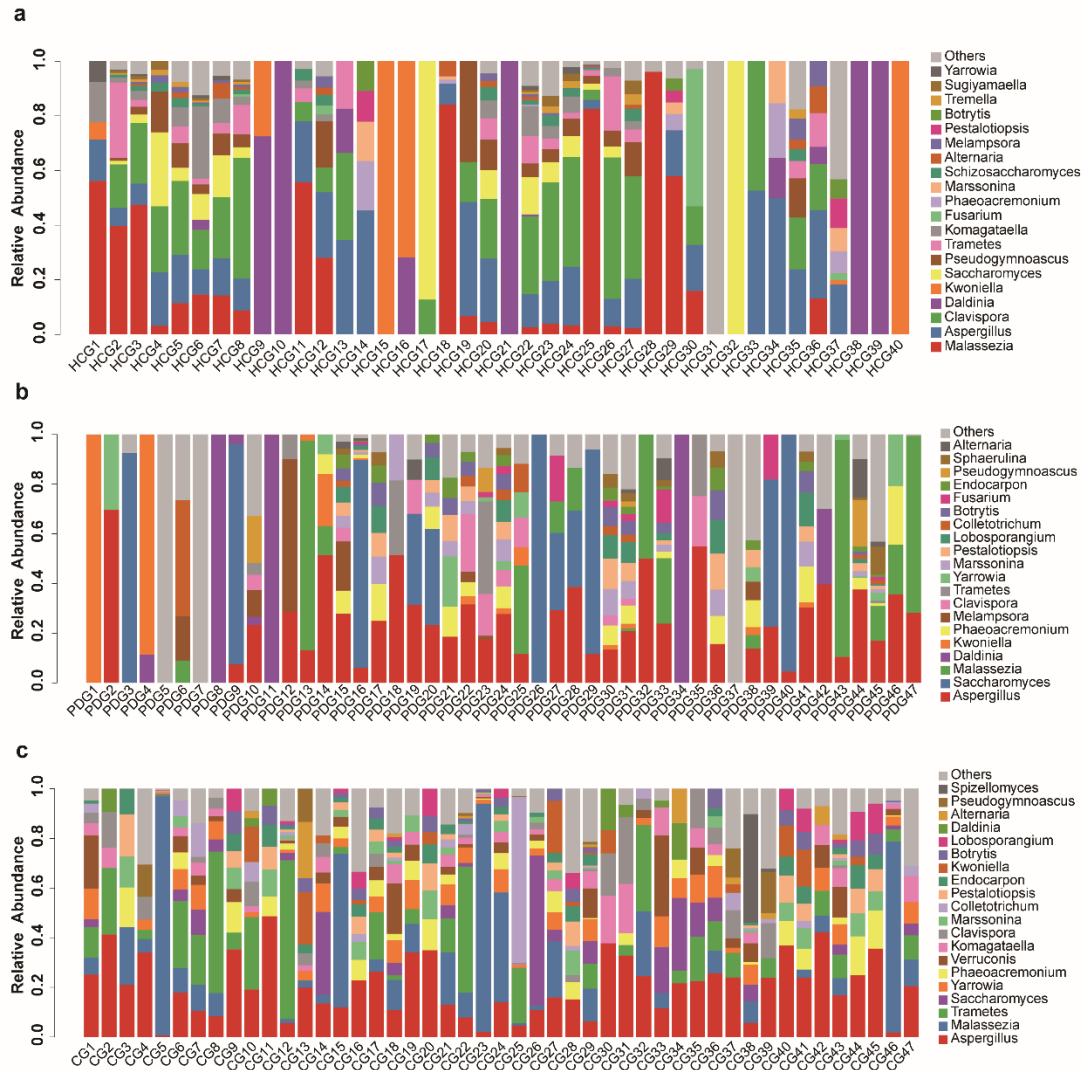
710 **groups. The colors represent different groups. PCoA1 and PCoA2 represent**

711 the top two principal coordinates that captured most of the diversity. The  
 712 fraction of diversity captured by the coordinate is valued as a percentage.



713  
 714 **Suppl.Fig.1 Oropharyngeal bacterial characterization of every subjects among**  
 715 **HCG, PDG and CG. Average compositions of relative abundance of the top20**  
 716 **bacterial communities for each group at the genus level, a for HCG, b for PDG**  
 717 **and c for CG. shared bacterial landscape on genus level among HCG, PDG**  
 718 **and CG group.**

719



720

721 **Suppl.Fig.1 Oropharyngeal fungal characterization of every subjects among**

722 **HCG, PDG and CG. Average compositions of relative abundance of the top20**

723 **fungal communities for each group at the genus level, a for HCG, b for PDG**

724 **and c for CG. shared bacterial landscape on genus level among HCG, PDG**

725 **and CG group.**

726

# Figures

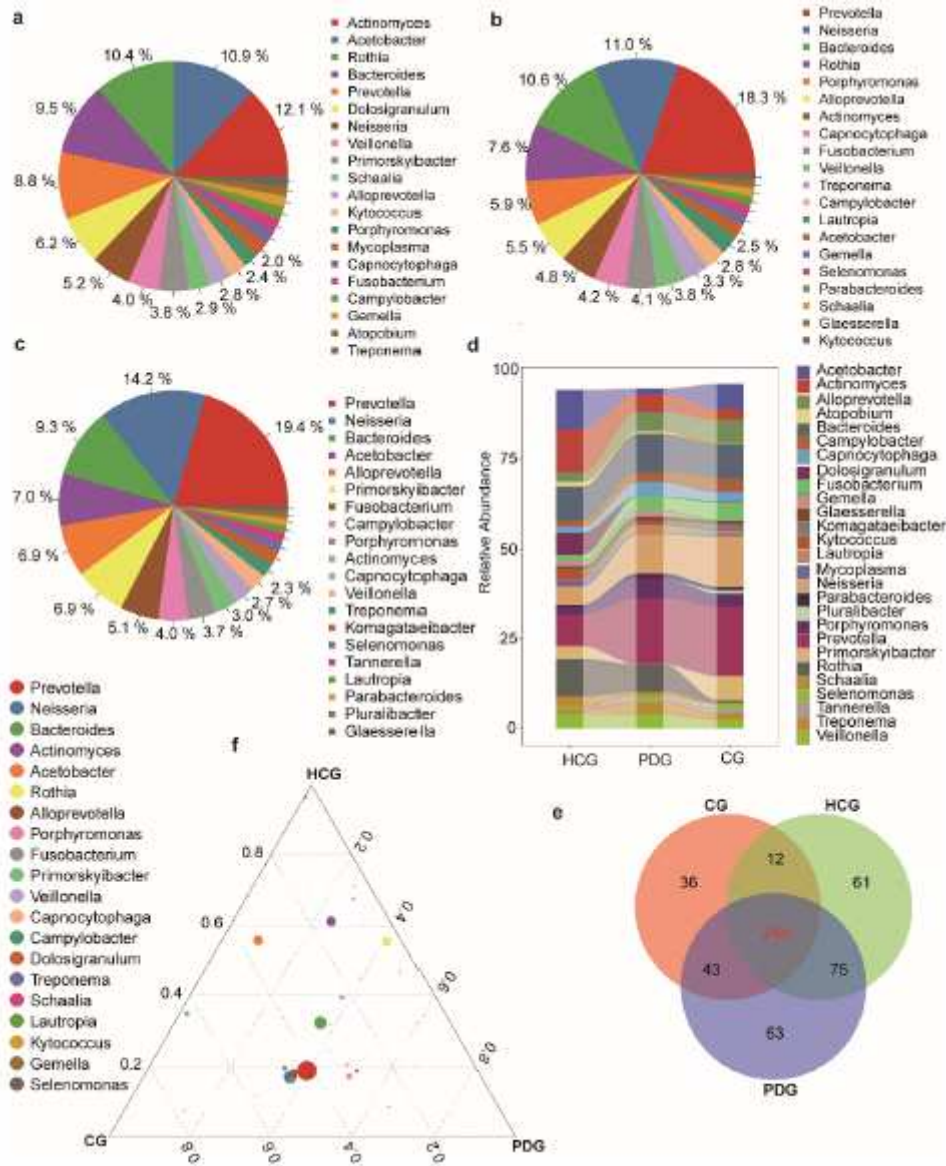


**Figure 1**

Oropharyngeal bacterial characterization and alterations among HCG, PDG and CG. Average compositions of relative abundance of the top20 bacterial communities for each group at the genus level, a for HCG, b for PDG and c for CG. d Alterations of top20 bacterial communities among the three groups at the genus level, Especially, Prevotella is significantly higher in PDG than that in HCG (Wilcoxon rank-sum test,  $p < 0.001$ ). e Venn diagram showing shared and unique genus of the three groups. f Ternary plots depicting the 244 shared bacterial landscape on genus level among HCG, PDG and CG group. The sum of the proportion for one specific bacteria in the three groups was set as 1, and the proportion of one

specific bacteria in each group is equal to its as 1, and the proportion of one specific bacteria in each group is equal to its corresponding relative abundance divided by the relative abundance sum of corresponding relative abundance divided by the relative abundance sum of this bacteria in the three groups. The sizethis bacteria in the three groups. The size of the circles represents the relative of the circles represents the relative abundance of the genus.abundance of the genus.

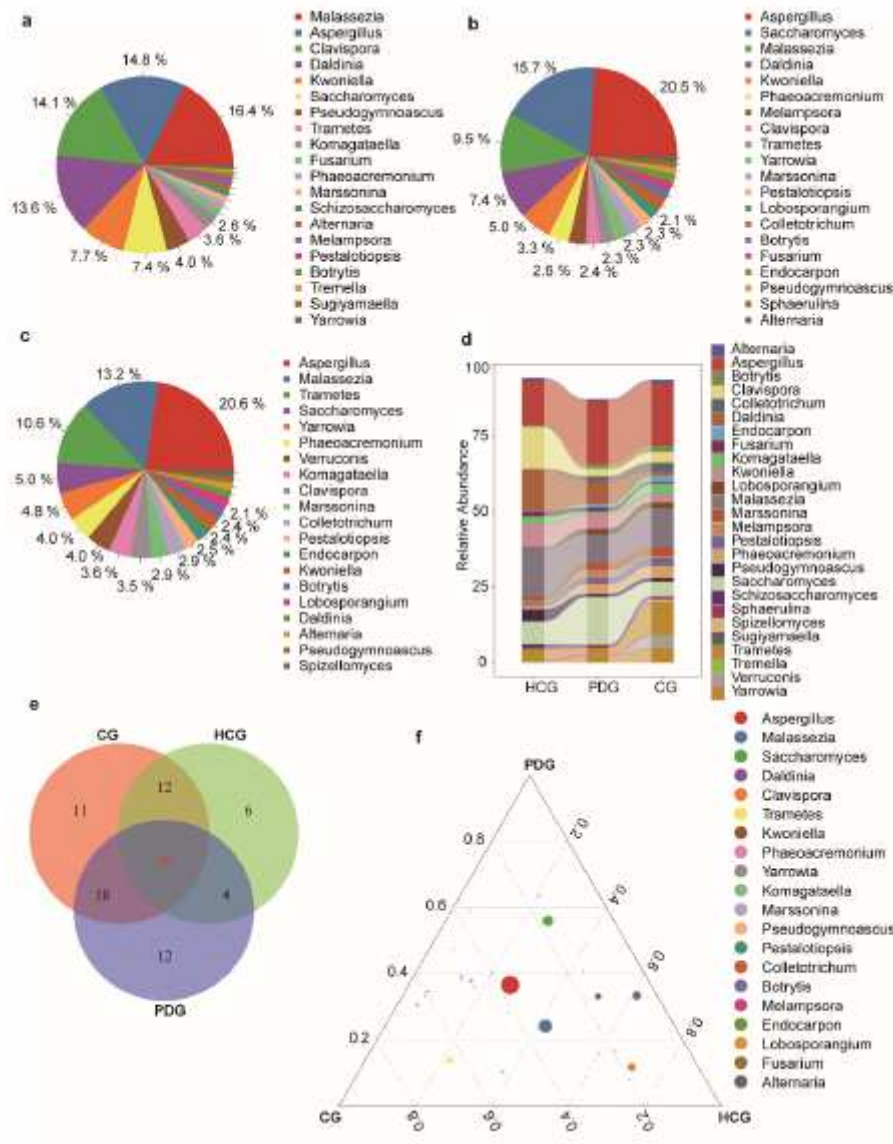


**Figure 2**

Oropharyngeal fungal characterization and alterations among HCG, PDG and CG. Average compositions of relative abundance of the top20 fungal communities for each group at the genus level, a for HCG, b for PDG and c for CG. d Alterations of top20 fungal communities among the three groups at the genus level. e Venn diagram showing shared and unique genus of the three groups. groups. ff Ternary plots depicting the 244 shared fungal landscape on genus level among HCG, PDG and CG group. The sum of the proportion for one level among HCG, PDG and CG group. The sum of the proportion for one specific bacteria in the three groups was set as 1, and the proportion of one specific bacteria in the three groups was set as 1, and the

proportion of one specific fungi in each group is equal to its corresponding relative abundance in each group is equal to its corresponding relative abundance divided by the relative abundance sum of this fungi in the three groups. The size of the circles represents the relative abundance of the genus. The size of the circles represents the relative abundance of the genus.

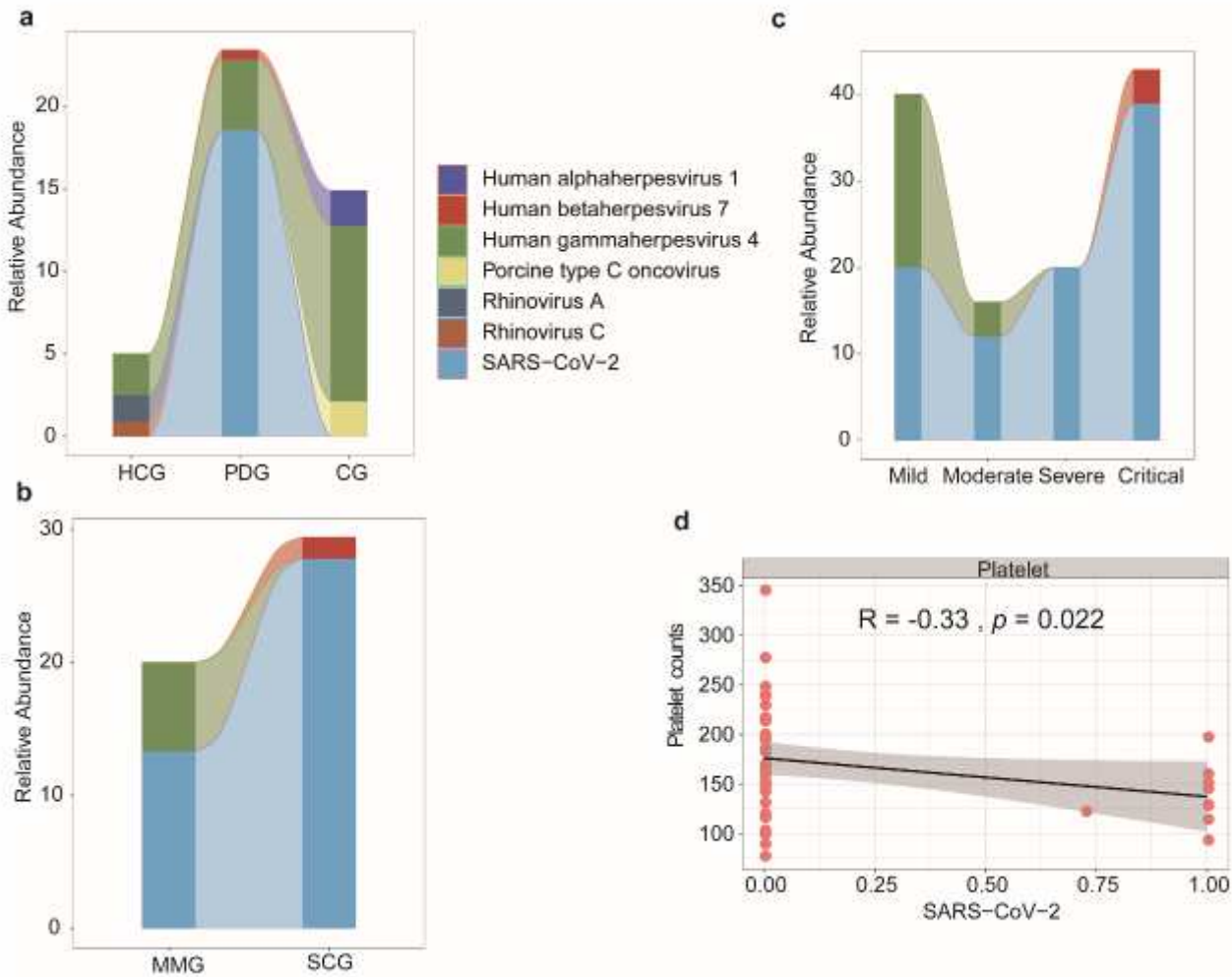


**Figure 3**

Oropharyngeal SARS CoV 2 viral load was positively correlated with the severity of COVID 19. a The relative abundance changes of 7 oropharyngeal viral species (including SARS-COR-2) among HCG, PDG and CG group, b among MMG and SCG group, c among Mild, Moderate, Severe and Critical group. d Negative correlation between SARS-CoV-2 viral load (x-axis) and platelet counts (y-axis) (Spearman correlation analysis:  $R = -0.330$ ,  $P = 0.022$ ), Linear regression lines are shown in each scatter plot in black, and shaded regions represent 95% confidence intervals.

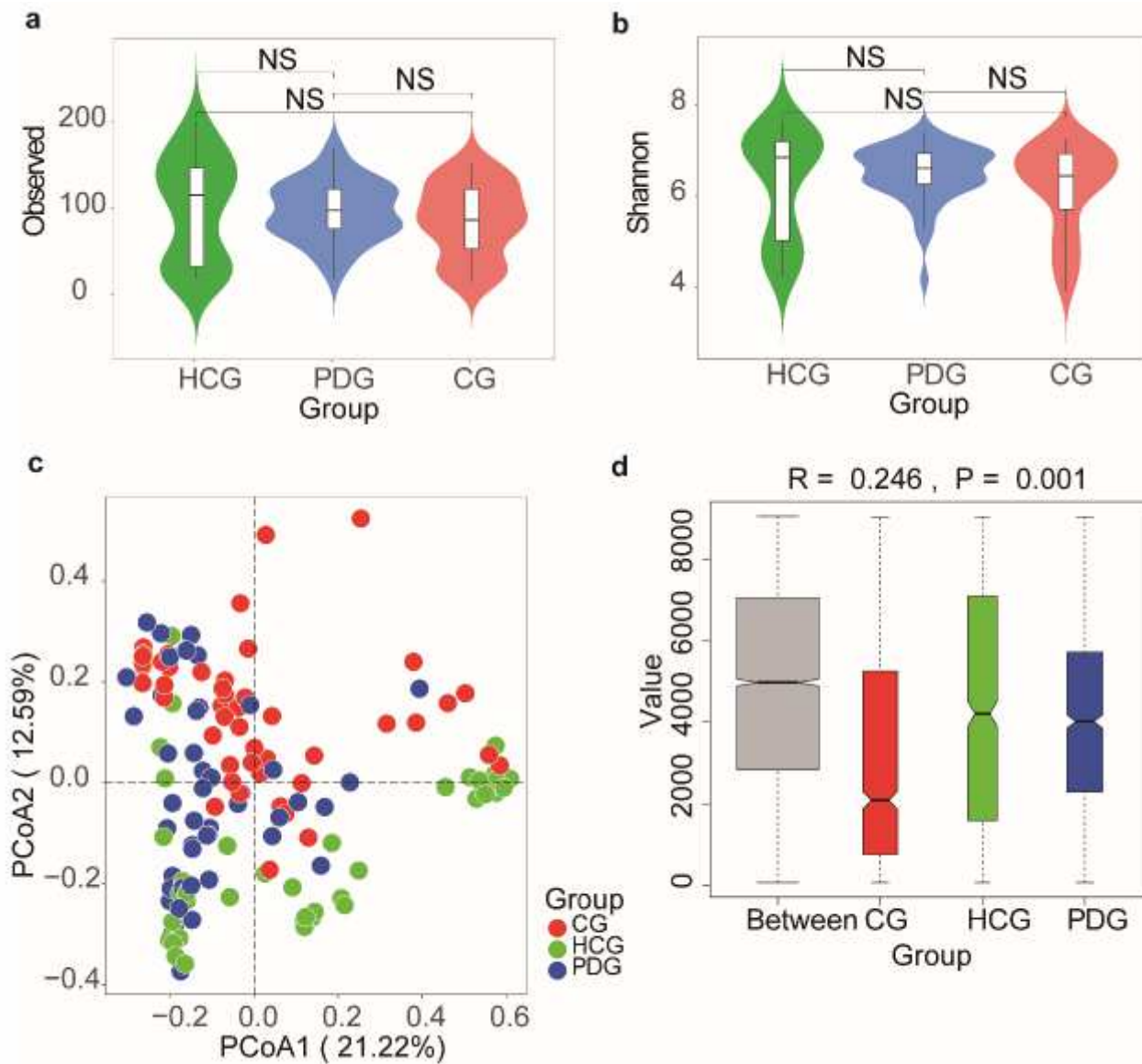


**Figure 4**

Oropharynx microbial alterations in diversity among HCG, PDG and CG. a Little changes in Observed index among HCG, PDG and CG (NS: P 0.05). b Little changes in Shannon index among HCG, PDG and CG (NS: P 0.05). c Principal coordinate analysis (PCoA) of Bray-Curtis distance showed obviously changes in  $\beta$  diversity among HCG, PDG and CG. The colors represent three different groups. PCoA1 and PCoA2 represent the top two principal coordinates that captured most of the diversity. The fraction of diversity captured by the coordinate is valued as a percentage. coordinate is valued as a percentage. dd. The analysis of similarities (ANOSIM). The analysis of similarities (ANOSIM) based on Bray-Curtis distance shows that  $R > 0$  and  $P < 0.05$ , indicating that the inter-group difference among HCG, PDG and CG was greater than the intra-group difference in each group. The R means the statistical value of ANOSIM, group difference in each group. The R means the statistical value of ANOSIM, y-axis value means Bray-Curtis rank, and 999 was

used for the permutations. Curtis rank, and 999 was used for the permutations. NSNS means no significant. means no significant.

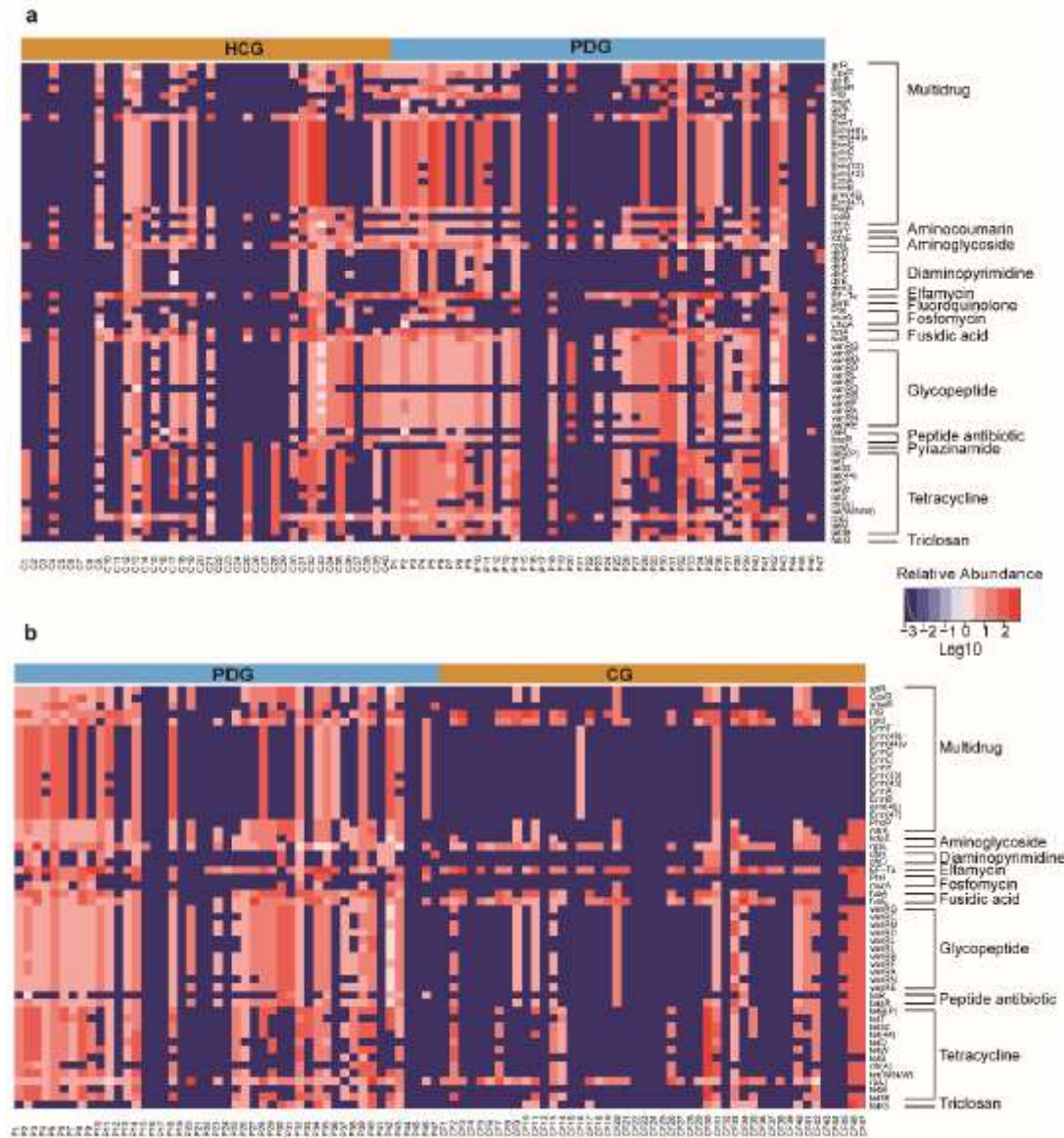


**Figure 5**

Obviously changes of oropharynx microbial antibiotic resistance genes expression among HCG, PDG and CG. a expression among HCG, PDG and CG. a Heatmap for the relative abundances Heatmap for the relative abundances of microbial antibiotic resistance genes expression between HCG and PDG. of microbial antibiotic resistance genes expression between HCG and PDG. bb Heatmap Heatmap for the relative abundances of microbial antibiotic resistance genes for the relative abundances of microbial antibiotic resistance genes expression between PDG and CG. The relative abundance changes from low expression between PDG and CG. The relative abundance changes from low to high is showed by color changes from blue to red. The log10 value was used to high is showed by color changes from blue to red. The log10 value was used to show the abundance ofto show the abundance of antibiotic reantibiotic resistance genesistance gene..

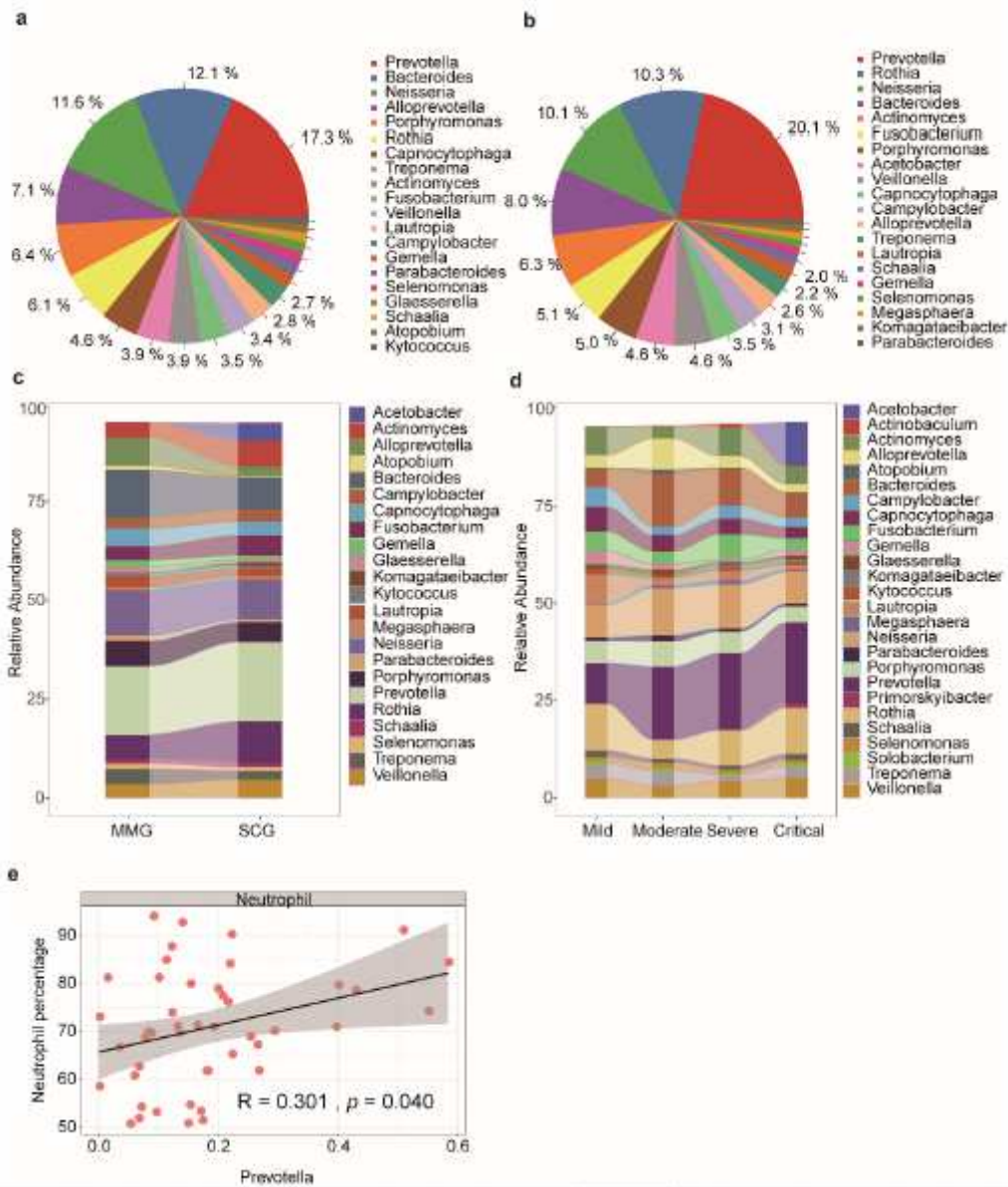


**Figure 6**

Alterations of oropharyngeal bacteria reflected disease severity in patients with COVID 19. a, b Average compositions of relative abundance of the top20 bacterial communities of MMG and SCG groups at the genus level. c Alterations of top20 bacterial communities among the MMG and SCG groups at the genus level. d Alterations of top20 bacterial communities among the Mild, Moderate, Severe and Critical groups at the genus level. Especially, the alteration of Prevotella gradually increased along with the symptom aggravated in patients with COVID 19. e Positive correlation between Prevotella relative abundance (x-axis) and the elevation of Neutrophil percentage (y-axis) (Spearman correlation analysis:  $R = 0.301$ ,  $p = 0.040$ ), Linear regression lines are shown in each scatter plot in black, and shaded regions represent 95% confidence intervals

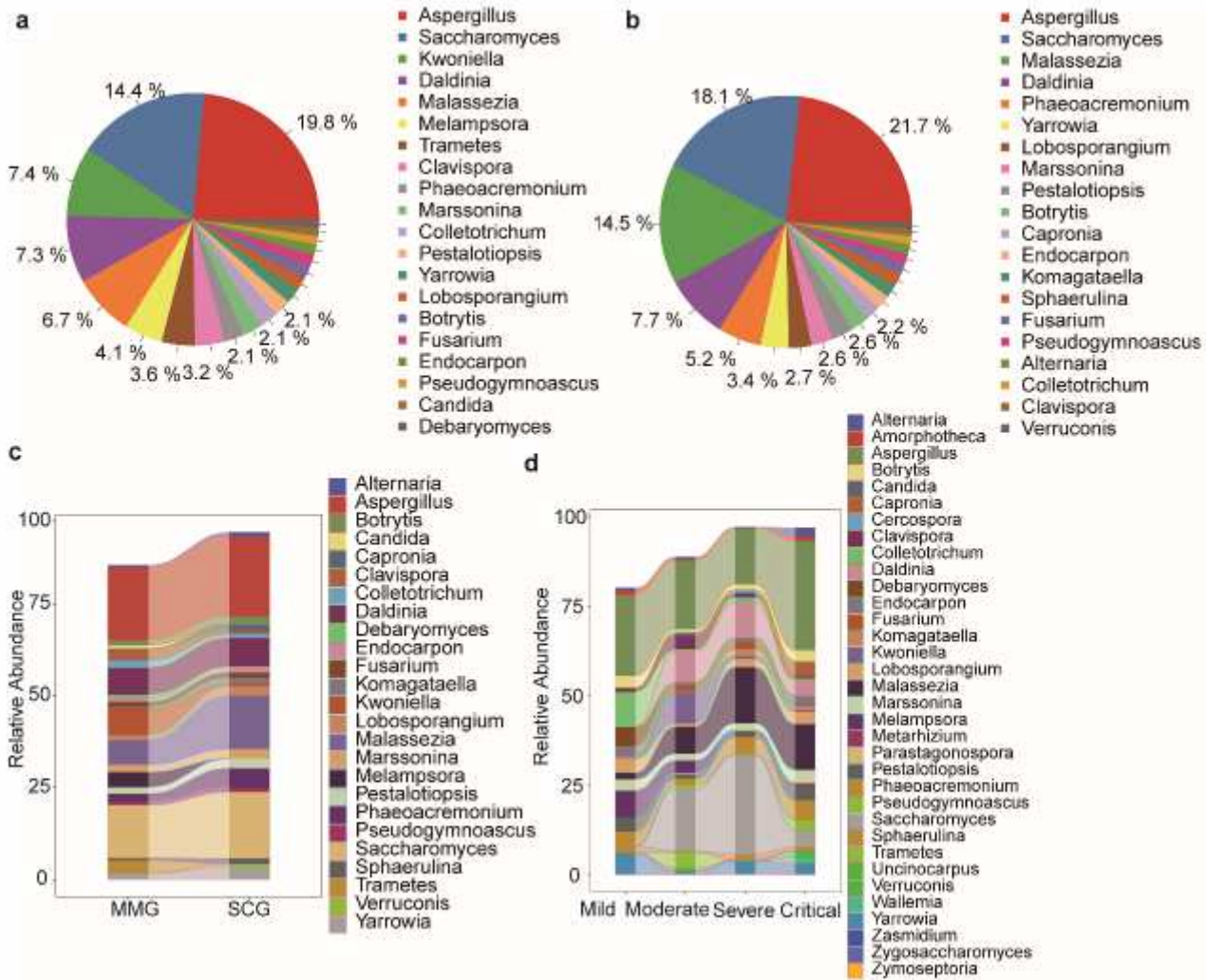


**Figure 7**

Alterations of oropharyngeal fungi reflected disease severity in patients with COVID 19. a, b Average compositions and relative abundance of the top20 fungal communities of MMG and SCG groups at the genus level. c Alterations of top20 fungal communities among the MMG and SCG groups at the genus level. d Alterations of top20 fungal communities among the Mild, Moderate, Severe and Critical groups at the genus level. Especially *Aspergillus* increased remarkably in critical Patients with COVID 19.

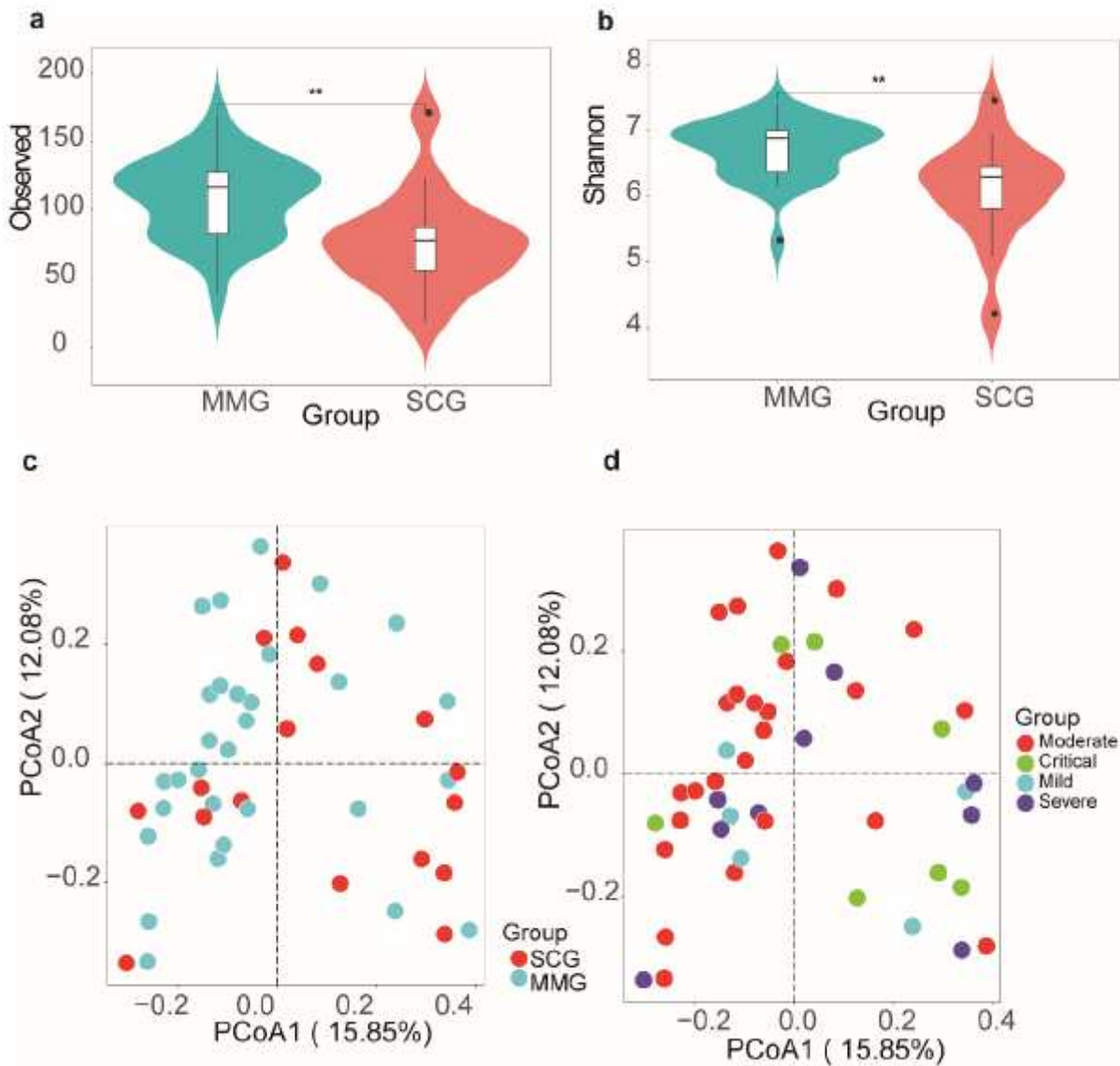


**Figure 8**

Decreased oropharyngeal microbiome in diversity appeared to be associated with COVID 19 severity. a Obviously decreased oropharyngeal microbiome in Observed index between MMG and SCG (\*\*: P 0.001). b Obviously decreased oropharyngeal microbiome in Shannon index between MMG and SCG (\*\*: P 0.001). c Principal coordinate analysis (PCoA) of Bray Curtis distance showed obviously changes in  $\beta$  diversity among MMG and SCG groups. d Principal coordinate analysis (PCoA) of Bray Curtis distance showed obviously changes in  $\beta$  diversity among Mild, Moderate, Severe and Critical groups. The colors represent different groups. PCoA1 and PCoA 2 represent the top two principal coordinates that captured most of the diversity. The the top two principal coordinates that captured most of the diversity. The fraction of diversity captured by the coordinate is valued as a percentage. fraction of diversity captured by the coordinate is valued as a percentage.

## Supplementary Files

This is a list of supplementary files associated with this preprint. Click to download.

- [FigS1.png](#)